Natural convection heat transfer between a fixed array of cylinders and its cubical enclosure
by Gordon Crupper

A thesis submitted in partial fulfillment of the requirements for the degree of MASTER OF SCIENCE
in Mechanical Engineering
Montana State University
© Copyright by Gordon Crupper (1977)

Abstract:
Natural convection heat transfer from a fixed array of four isothermal , heated cylinders to an isothermal, cooled cubical enclosure was experimentally investigated for both a horizontal and vertical position of the array. The cylinders were arranged in a square array and four test fluids (air, water, 99% aqueous glycerin, and a silicone oil) yielding Prandtl numbers in the range of 0.7 to 3.1 x 10^4 were used with each geometric position.

The heat transfer results are presented in correlation equations for each fluid and geometry as well as an overall correlation utilizing all data. Several equation forms were used in which the Nusselt number was correlated as a function of combinations of the Rayleigh, Prandtl, and Grashof numbers. The best equation found to correlate all data with a single parameter was NuB = 0.286 RaB 0.275 using the boundary layer length as a characteristic dimension. This equation provided results with a 9.30% average deviation. The results were compared with equations developed for single bodies to cubical and spherical enclosures for the same Prandtl number range. Correlations of the data are provided in tabular form for all fluids and geometries.

Several geometric effects were observed. The vertical configuration convected less heat than the horizontal while a rotation about the vertical axis for each of these configurations had negligible effect. The resulting decrease in heat transfer for the vertical configuration was attributed to a complex interaction between the boundary layer length, the flow patterns which resulted from the geometry, and the cross sectional area exposed to the upward flow. As the Prandtl number of the fluid media increased it tended to damp out the geometric effects. Flow visualization studies and temperature profiles were used to aid in evaluating the geometric effects.

STATEMENT OF PERMISSION TO COPY

In presenting this thesis in partial fulfillment of the requirements for an advanced degree at Montana State University, I agree that the Library shall make it freely available for inspection. I further agree that permission for extensive copying of this thesis for scholarly purposes may be granted by my major professor, or, in his absence, by the Director of Libraries. It is understood that any copying or publication of this thesis for financial gain shall not be allowed without my written permission.

Signature 

Date MAY 27, 1977

NATURAL CONVECTION HEAT TRANSFER BETWEEN A FIXED ARRAY OF CYLINDERS AND ITS CUBICAL ENCLOSURE

by

GORDON CRUPPER, JR.

A thesis submitted in partial fulfillment
of the requirements for the degree

of

MASTER OF SCIENCE

in

Mechanical Engineering

Approved:

Chairperson, Examining Committee

Head, Major Department

Graduate Dean

MONTANA STATE UNIVERSITY
Bozeman, Montana

May, 1977

ACKNOWLEDGMENT

The author expresses his appreciation to all those who have aided in his work. Special appreciation is extended to Dr. Robert O. Warrington, Jr. for his guidance and counsel during the preparation of this thesis and also to Dr. J. A. Scanlan, Dr. T. C. Reihman, and Dr. R. L. Mussulman for their advice and instruction. The author is especially appreciative of the patience and understanding of his wife and children.

The work in this thesis was supported by the United States Army under the Advance Degree Program for ROTC Instructor Duty.

TABLE OF CONTENTS

Chapter	Page
VITA	ii
ACKNOWLEDGMENT	iii
LIST OF TABLES	v
LIST OF FIGURES	vi
ABSTRACT	viii
NOMENCLATURE	ix
I. INTRODUCTION	1
II. LITERATURE REVIEW	3
III. EXPERIMENTAL APPARATUS AND PROCEDURE	13
IV. DISCUSSION OF RESULTS	24
V. CONCLUSIONS AND RECOMMENDATIONS	65
APPENDIX I	69
APPENDIX II	75
BIBLIOGRAPHY	80

LIST OF TABLES

Table		Page
4.1	Ranges of the Dimensionless Parameters	25
4.2	Correlation Equations for Air All	48
4.3	Correlations for Glycerin Data	50
4.4	Correlations for Water Data	54
4.5	Correlations for Silicone Data	57
4.6	Correlations for All Data	59
4.7	Fit of Data to Previously Developed Equations	64

LIST OF FIGURES

Figure		Page
3.1	Heat Transfer Apparatus	14
3.2	Single Cylinder with Heat Tape Installed	17
3.3	Inner Body Partially Assembled	17
4.1	Nu_L versus Gr_L for All Data	28
4.2	Flow Pattern for Horizontal Cylinders with 20 cs Fluid and ΔT = 10.71K	31
4.3	Flow Pattern Around Upper Horizontal Cylinder with 20 cs Fluid and ΔT = 10.71K	32
4.4	Flow Pattern Around Lower Horizontal Cylinder with 20 cs Fluid and ΔT = 10.71K	33
4.5	Flow Pattern Around Center Support Sphere with 20 cs Fluid and ΔT = 10.71K	34
4.6	Flow Pattern for Horizontal Cylinders with 20 cs Fluid and ΔT = 54.43K	35
4.7	Flow Pattern for Horizontal Cylinders with Air and ΔT = 7.67K	36
4.8	Flow Pattern for Horizontal Cylinders with Air and ΔT = 21.61K	37
4.9	Flow Pattern for Vertical Cylinders with Air and T = 17.01K	38
4.10	Nu_L versus Gr_L FOR 0° and 45° Rotations with the Cylinders in the Horizontal Position	40
4.11	Nu_L versus Gr_L FOR 0° and 45° Rotations with the Cylinders in the Vertical Position	41
4.12	Temperature Profile for Rotation About the Vertical Axis with Silicone-Horizontal Position	42

Figure		Page
4.13	Temperature Profile for Rotation About the Vertical Axis with Silicone-Horizontal Position.	43
4.14	Temperature Profile for Rotation About the Vertical Axis with Glycerin-Vertical Position	44
4.15	Nusselt Number versus Rayleigh Number for Air Data with Correlation Equations Superimposed	47
4.16	Nusselt Number versus Rayleigh Number for Glycerin Data with Correlation Equations Superimposed.	52
4.17	Nusselt Number versus Rayleigh Number for Water Data with Correlation Equations Superimposed	55
4.18	Nusselt Number versus Rayleigh Number for Silicone Data with Correlation Equations Superimposed.	56
4.19	Nu_L versus Gr_L for All Data with Correlation Equations Superimposed	61
4.20	Nu_B versus Gr_B for All Data with Correlation Equations Superimposed	62
I.1	Flow Pattern Between Cylinders in the Vertical Position. .	71
I.2	Steady-State Heat Balance for the Support Sphere	73

ABSTRACT

Natural convection heat transfer from a fixed array of four isothermal, heated cylinders to an isothermal, cooled cubical enclosure was experimentally investigated for both a horizontal and vertical position of the array. The cylinders were arranged in a square array and four test fluids (air, water, 99% aqueous glycerin, and a silicone oil) yielding Prandtl numbers in the range of 0.7 to 3.1 x 10^4 were used with each geometric position.

The heat transfer results are presented in correlation equations for each fluid and geometry as well as an overall correlation utilizing all data. Several equation forms were used in which the Nusselt number was correlated as a function of combinations of the Rayleigh, Prandtl, and Grashof numbers. The best equation found to correlate all data with a single parameter was

$$Nu_B = 0.286\ Ra_B 0.275$$

using the boundary layer length as a characteristic dimension. This equation provided results with a 9.30% average deviation. The results were compared with equations developed for single bodies to cubical and spherical enclosures for the same Prandtl number range. Correlations of the data are provided in tabular form for all fluids and geometries.

Several geometric effects were observed. The vertical configuration convected less heat than the horizontal while a rotation about the vertical axis for each of these configurations had negligible effect. The resulting decrease in heat transfer for the vertical configuration was attributed to a complex interaction between the boundary layer length, the flow patterns which resulted from the geometry, and the cross sectional area exposed to the upward flow. As the Prandtl number of the fluid media increased it tended to damp out the geometric effects. Flow visualization studies and temperature profiles were used to aid in evaluating the geometric effects.

NOMENCLATURE

Symbol	Description
A	Total heat exchanger area
A_c	Total area of the cylinders
B	Distance traveled by the boundary layer on the inner body
c_p	Specific heat at constant pressure
f	Denotes function
g	Acceleration of gravity, 9.81 m/sec^2
Gr_x	Grashof number, defined by equation (2.2)
Gr_x^*	Local Grashof number, $g\beta q x^4/k\nu^2$
h	Average heat transfer coefficient, $Q_{CONV}/A_c\Delta T$
k	Thermal conductivity
L	Gap width or hypothetical gap width, R_o-R_i
l	Length of straight cylindrical section
Nu_x	Nusselt number, hx/k, where x is any characteristic dimension
Pr	Prandtl number, $c_p\mu/k$
Q_{COND}	Heat transfer by conduction
Q_{CONV}	Heat transfer by convection
$Q_{RADIATION}$	Heat transfer by radiation
R	Local position of thermocouple probe
Ra_x	Rayleigh number, $\rho^2 g\beta(T_i-T_o)x^3 c_p/\mu k$, where x is any characteristic dimension

Symbol	Description
Ra_x^*	Modified Rayleigh number, $Ra_x(L/R_i)$
$R_{i(o)}$	Inner(outer) body hypothetical radius equal to the radius of a sphere having an equal volume
R_{ND}	Dimensionless radius defined as $R/R(\theta)$
$R(\theta)$	Length of probe for radial position θ
T	Local temperature
T_f	Film temperature, $T_f = (T_w + T_\infty)/2$
T_{ND}	Dimensionless temperature defined as, $(T-T_0)/(T_I-T_0)$
$T_{I(O)}$	Temperature of the inner(outer) body
T_W	Temperature at the outer surface of any body
$TMVL_{I(O)}$	Temperature of the inner(outer) body as measured by the thermocouple in millivolts
T_s	Temperature of the support sphere
T_∞	Temperature of the ambient, far from the inner body
x	Any characteristic dimension
β	Thermal expansion coefficient
μ	Dynamic viscosity
ν	Kinematic viscosity
Π	Ratio of circumference of a circle to the diameter, 3.14159
θ	Temperature probe angular location as defined on page 15
ρ	Density

CHAPTER 1

INTRODUCTION

Investigation in the area of heat transfer by natural convection within enclosures has increased dramatically in the last decade. This has been in response to advances in electrical packaging, solar heating technology, and increased demands for handling nuclear waste. Most recently the demands for energy conservation have increased the importance for a better understanding of natural convection within enclosures.

The purposes of this study are to determine the heat transferred between a set of four isothermal, heated cylinders (multiple bodies) and an isothermal, cooled cubical enclosure, to determine the effect of the position of the tubes within the enclosure, and to compare the results with the findings of previous studies on heat transfer from single bodies to the same form of enclosure. Four fluids and inner body positions are utilized in studying the heat transferred. The body positions include the set of cylinders in both a horizontal and vertical position and include a 45 degree rotation about the vertical axis for each position. The fluids used are air, water, 99 percent glycerin, and a Dow-Corning 20 cs fluid. The fluids provide a Prandtl number range of 0.7 to 31,000.

Although the heat transfer problem is coupled with a fluid-flow problem, the intent of this study is directed primarily toward the heat transfer problem. Flow visualization and temperature profiles within

the enclosure are obtained to aid in evaluating the heat transfer.

CHAPTER II

LITERATURE REVIEW

Heat transfer by natural convection is a field in which several subdivisions are evident. The majority of the initial studies dealt solely with heat transfer from common shapes (e.g. plates, cylinders, spheres, etc.) to a sufficiently large surrounding fluid medium as to be termed an infinite atmosphere. Further developments found a need to study the natural convective heat transfer from one body to an enclosing body through a fluid medium that could not be treated as infinite. Both of the major subdivisions mentioned above have experienced emphasis on the separate areas of heat transfer from single bodies, series of like shapes usually symmetrically placed, and other geometric effects as well as specialized fluid properties. For purposes of clarity this discussion will be covered in two phases. These are (1) natural convection to an infinite atmosphere, and (2) natural convection in enclosures.

NATURAL CONVECTION TO AN INFINITE ATMOSPHERE

There have been many major developments in research into the heat transferred from a single geometric shape to an infinite atmosphere. Several texts provide an excellent summary of these advances. McAdams [1] provides a comprehensive review of earlier results of investigations into natural convection heat transfer from single horizontal cylinders to an infinite atmosphere with Rayleigh numbers ranging from 10^{-4} to 10^{9}. Both Gebhart [2] and Holman [3] provide excellent references for the heat transfer from horizontal and

vertical cylinders with Rayleigh numbers from 10^{-5} to 10^{12}, well into the turbulent region.

In nearly all cases three dimensionless parameters are utilized to correlate the heat transfer by natural convection. The resulting equation is of the form

$$Nu_x = f(Gr_x , Pr) \tag{2.1}$$

in which the dimensionless parameters are defined as

$$Gr_x = \frac{g\beta(T_w - T_\infty)\, x^3}{\nu^2} \tag{2.2}$$

$$Nu_x = \frac{hx}{k} \tag{2.3}$$

and

$$Pr = \frac{c_p \mu}{k} \tag{2.4}$$

where x is a characteristic length. Simplification of the correlating equation has been accomplished by combining the Grashof number (Gr_x) and the Prandtl number (Pr) to form a single dimensionless parameter, the Rayleigh number, as follows:

$$Ra_x = Gr_x \cdot Pr \tag{2.5}$$

The equation form most commonly utilized to correlate heat transfer

data is

$$Nu_x = C_1 (Gr_x Pr)^{C_2} \tag{2.6}$$

Fujii and Fujii [4], Roy [5], and Churchill and Ozoe [6] present studies to express C_1 explicitly as a function of the Prandtl number in the equation

$$Nu_x = C_1 (Gr_x^* Pr)^{1/5} \tag{2.7}$$

for laminar flow along vertical surfaces with uniform heat flux. The results were satisfactory, but are limited in application to this particular situation.

Lienhard [7] presented theoretical arguments that regardless of shape, the overall heat transfer correlation in the laminar range can be expressed as

$$(Nu_x/Ra_x)^{1/4} \simeq 1/2 \tag{2.8}$$

for wholly immersed isothermal bodies. He recommended that this relationship be used with the length of travel of the boundary layer as the characteristic length (x) to achieve results varying only by a few percent.

Eckert and Soehngen [8] researched the effects of a vertical series of horizontal cylinders upon each other. Utilizing 2.231 cm diameter, isothermal cylinders, they observed that when two cylinders were

utilized, one directly over the other at a distance of four diameters, there was no change in the Nusselt number of the lowest cylinder as opposed to a single cylinder. However, the upper cylinder evidenced a reduction in heat transferred. The resulting Nusselt number of the upper cylinder was 87 percent of the lower cylinder. Similar results were achieved when the series was increased to three cylinders. The Nusselt numbers were 100, 83, and 65 percent, respectively, from bottom to top cylinders. When the middle cylinder was moved laterally out of line by one half a diameter, the Nusselt number of that cylinder rose to 103 percent of the bottom cylinder while that of the top cylinder was 86 percent.

Eckert and Soehngen reasoned that the effect of the warmer wake around the upper tubes reduced the heat transferred since the temperature differential had decreased. Conversely, the staggered tube was not in the natural convection plume and an induced fluid movement of cooler air resulted in a greater capacity to transfer heat. Analysis of the method of heat transfer from the top cylinder in the staggered array was more complex as it was effected by both the induced wake and the convective plume.

Leiberman and Gebhart [9], in 1968, investigated the interactions between the natural convective flows of several closely spaced surfaces by using long, horizontal wires in a parallel array at several spacings and inclinations. Other investigations which include temperature and

velocity measurements about a line source have been conducted by Brodowicz and Kierkus [10], and Forstrom and Sparrow [11]. All of the above investigators found that cool air is induced into the plume from the sides and below the source.

The influence of tube spacing and array on natural convection heat transfer coefficients for horizontal tube bundles has been determined experimentally by Tillman [12]. Five pitch to diameter (P/D) ratios were studied for a square array of 16 tubes, and four (P/D) ratios were studied for a staggered array of 14 tubes. The following equations were developed to correlate the data:

$$Nu_f = 0.057\ (Gr\ Pr)_f^{0.5} \tag{2.9}$$

for square arrays, and

$$Nu_f = 0.067\ (Gr\ Pr)_f^{0.5} \tag{2.10}$$

for staggered arrays, where the thermal properties of the fluid were evaluated at the film temperature

$$T_f = \frac{T_2 + T_\infty}{2} \tag{2.11}$$

except β which was evaluated at the ambient temperature. The characteristic dimension was defined as

$$D_h = \frac{4\ A_c x}{A} \tag{2.12}$$

in which A_c is the flow cross section area, A is the total heat exchanger area, and x is the height of the tube bundle. Conclusions drawn by Tillman indicate that tube spacing has more effect on the heat transfer than the type of array. Also, an optimum spacing for each array was determined for separate temperature differentials.

Natural convection from vertical tube bundles has been researched by Davis and Perona [13]. They utilized 42 tubes having an outside diameter of 1.58 cm and a length of 1.23 cm arranged in 7 staggered rows of 6 tubes per row. Experimental results were compared with theoretical results obtained from a finite difference solution of the problem. The results obtained from both experimental data and theoretical calculations correlated extremely well with the exception of the values in the region where the end support system had an apparent influence.

NATURAL CONVECTION IN ENCLOSURES

Natural convection in enclosures, in this discussion, will be restricted to heat transferred from one body or bodies completely enclosed by a second body. With this restriction imposed, one finds an area of investigation that has barely been initiated. The primary emphasis to date has been with single bodies geometrically centered within a second enclosing body.

As discussed previously, several dimensionless parameters were utilized in correlating the heat transfer data for natural convection

to an infinite atmosphere. Although these parameters remain valid for enclosures, a third element was found helpful, if not necessary, which alters equation (2.1) to the form

$$Nu_x = f(Gr_x , Pr , N_d) \tag{2.13}$$

where N_d is a ratio of characteristic dimensions.

There are several sources of information on heat transfer from a single body to its enclosure. Most recently, Warrington [14] developed equations from experimental data which are useful in correlating heat transfer between inner bodies utilizing spheres, cubes, and cylinders of varying sizes to both spherical and cubical enclosures using data obtained by Bishop [18], Scanlan, et al [19] and other major investigations, as well as considerable data of his own. The following correlation:

$$Nu_L = 0.396 Ra_L^{0.234} \left(\frac{L}{R_i}\right)^{0.496} Pr^{0.162}$$

was found to adequately describe the heat transferred for 9 different sizes of spherical, 11 cylindrical, and 6 cubical inner bodies when enclosed by a spherical or cubical outer body. Several different fluids were utilized to extend the Prandtl number range from 0.706 to 13,800. The average percent deviation was 13.50%. Correlations are also given for separate combinations of fluids, inner, and outer bodies. Warrington [14] also provides an exhaustive review of the literature

pertaining to heat transfer from a single geometric shape to its enclosure.

Kuehn and Goldstein [15] analytically developed a correlating equation for horizontal concentric cylinders. Utilizing the experimental results of eight studies by other authors in which the ratio of outer to inner cylindrical diameters (D_o/D_i) was 2 and 3, and a Prandtl number of 0.7, they found that the analytical model fit the data within a few percent. Included in this study were two major extensions to the concentric cylinder problem. First was an analytical determination of the gap width at which the solution was the same as that for a single cylinder. It was found that when $D_o/D_i > 360$ at $Ra_{Di} = 10^7$ and $D_o/D_i > 700$ at $Ra_{D_i} = 10^{-1}$, the heat transfer coefficient was within 5% of that for a single cylinder. The second extension of their analytical model was the solution to the problem of multiple cylinders contained in a single cylindrical enclosure. For this case the correlating equation became

$$Nu = \frac{2N}{\ln[\,1+2/Nu_i\,] - N\,\ln[1-2/Nu_o]} \tag{2.15}$$

where the Nusselt number of the inner tube boundary conditions is

$$Nu_i = [(0.518Ra_{D_i}^{1/4}[1+(\frac{0.0559}{Pr})^{3/4}]^{-5/12})^{15}+(0.1Ra_{D_i}^{1/3})^{15}]^{1/15} \tag{2.16}$$

and the outer tube Nusselt number is

$$Nu_o = \{([(\frac{2}{1-e^{-0.25}})^{5/3}+(0.587Ra_{D_o}^{1/4})]^{3/5})^{15}+(0.1Ra_{D_o}^{1/3})^{15}\}^{1/15} \quad (2.17)$$

for a set of N inner cylinders. This equation is expected to be valid for small numbers of inner tubes. Although the authors are not specific as to the term small, they leave the impression that more than 4 or 5 cylinders would result in error. No other heat transfer data could be found for this configuration and, therefore, it has not been tested for validity.

The study of vertical tube bundles in enclosures has been mainly within the low Prandtl number range (liquid metals). Dutton and Welty [16] researched the effects of cylinder spacing on the heat transferred from a vertical rod bundle in a vertical cylindrical enclosure utilizing liquid mercury as the fluid medium, Pr = 0.023, with a uniform heat flux applied to the rod bundle. Axial and radial temperature distributions were also measured. Results of this study showed that there is a strong dependence on cylinder spacing and that the equation form for use in studies at low Prandtl numbers should involve the dimensionless parameter product defined as

$$Gr_x^* \cdot Pr \equiv (g\beta q x^4/k\alpha^2) \quad (2.18)$$

where q is a uniform heat flux.

The study of natural convection in enclosures as evidenced by the

literature has increased in the last decade. That portion which includes the use of multiple bodies still lacks appreciable knowledge. This study is intended to provide an extension of this area.

CHAPTER III

EXPERIMENTAL APPARATUS AND PROCEDURE

EXPERIMENTAL APPARATUS

The apparatus for this investigation consisted of a water jacketed cubical outer body, cooling system, power source, and a four cylinder inner body with supporting elements. One outer body system was used to obtain heat transfer data and temperature profiles while a separate system was utilized to photograph flow patterns. The assembled outer body and peripheral components are shown in Figure 3.1.

The outer body in which tests were conducted to determine the heat transfer was constructed from 1.27 cm thick, type 6061 aluminum with an inner 26.67 cm cubical chamber. This was a jacketed design consisting of a separate 3.175 cm wide rectangular channel for each face of the cube. Access to the test chamber was provided through a 25.4 cm removable circular plate on the top inner face and a completely removable outer face. A closed system consisting of a chiller, pump, and storage reservoir provided water to cool the outer body.

The flow rate of cooling water through each channel was controlled by a valve which fed four inlet and outlet ports. This arrangement assured uniform flow along the entire face and also allowed the temperature of each face to be controlled independently in order to achieve an isothermal outer body. The temperature of the inner wall was monitored by 34 copper constantan thermocouples epoxied 0.3175 cm from the inner

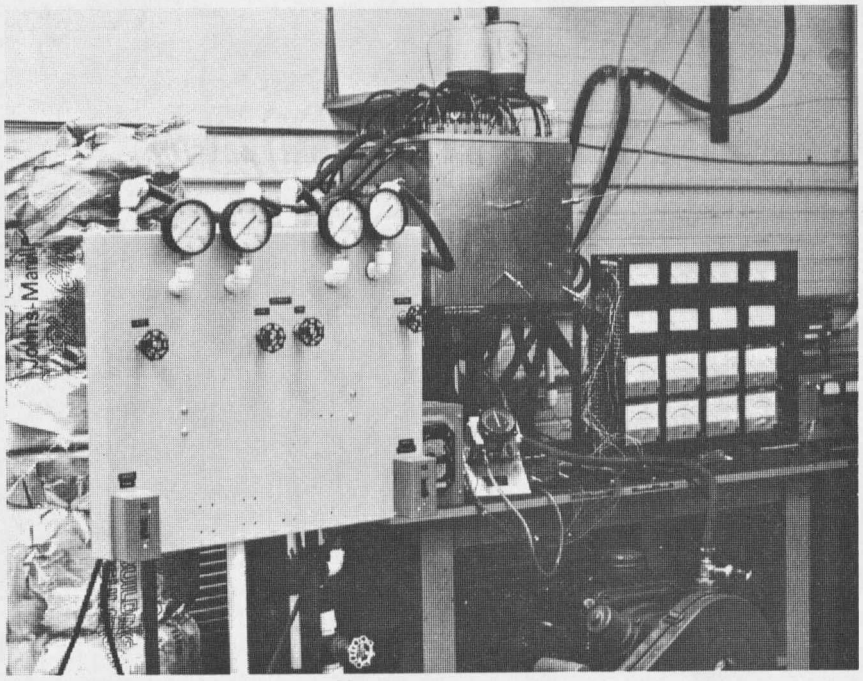


Figure 3.1 Heat Transfer Apparatus

face. The thermocouples for each face of the cube were connected in parallel which provided an average temperature for each face.. By controlling the flow of the cooling water, all faces could be maintained within 2 K.

To obtain temperature profiles within the test chamber, the outer body was designed with nine thermocouple ports. These consisted of one common and four additional ports on each of two separate axis. One axis was on a vertical plane through the center of the cube while the other was the vertical plane through the edge of the cube. The five ports in each axis were at 0°, 34°, 80°, 120°, and 160° measured downward from the top center vertical axis of the body. Each thermocouple port had a center tube which moved through a fixed port tube. The center tube was a 0.1587 cm diameter stainless steel tube which carried the copper-constantan thermocouple epoxied to the inner end. The outer sleeve was a 1.016 cm diameter stainless steel tube threaded into the inner jacket wall, and sealed in both jacket walls with rubber O-rings. The thermocouple lead tube was sealed within the sleeve by a Conax fitting attached to the outer end. A vernier caliper was modified to attach to the Conax fitting while the thermocouple tube was affixed to the sliding scale. This permitted the location of the thermocouple to be established with 0.0025 cm.

The outer body used for flow visualization was nearly identical to the one previously described. The major difference was that the

body was constructed from a clear polyvinyl and all portions were painted black except for a light source slot placed vertically on one side and one clear face which allowed photographs to be taken of the plane which was illuminated by the light source. An identical cooling system was installed and the monitoring and power devices were slaved from the heat transfer system.

The inner body design consisted of four identical cylinders and a supporting system which allowed it to be symmetrically centered in the inner body. Figures 3.2 and 3.3 show the inner body in different stages of construction. Copper tube (CDA #122) 17.78 cm long and 4.115 cm outside diameter was used to construct each cylinder. Each end of the tube was threaded and end caps were constructed from copper plate (CDA #110) to close the ends. In order to provide a support system, rods constructed from type 304 stainless steel 4.191 cm long and 0.9525 cm O.D. were threaded into each cylinder at its midlength and then connected to a 5.1 cm diameter polycarbonate sphere.

The resulting inner body configuration was four parallel cylinders in a square array 12.192 cm center to center. The final assembly was then placed symmetrically centered in the outer body supported by a main stem constructed from a 1.27 cm O.D. type 304 stainless steel rod. This support stem was designed to thread into the support sphere so that the entire tube system could be supported either on a horizontal or vertical axis with the unused tap being plugged when not in use. To

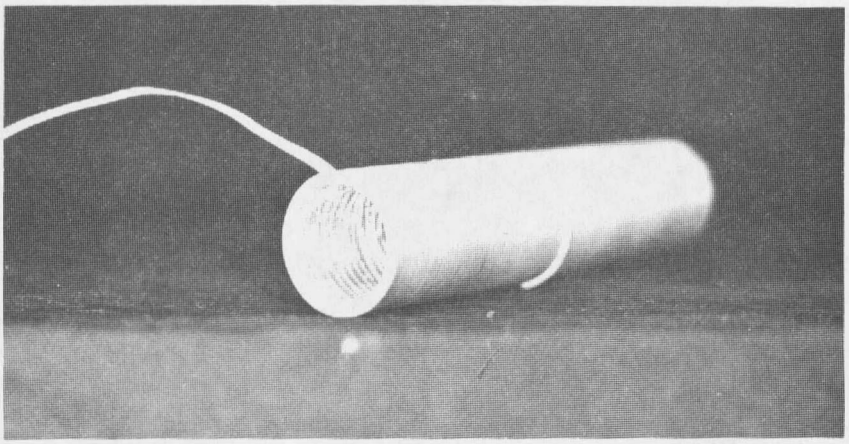


Figure 3.2 Single Cylinder with Heat Tape Installed

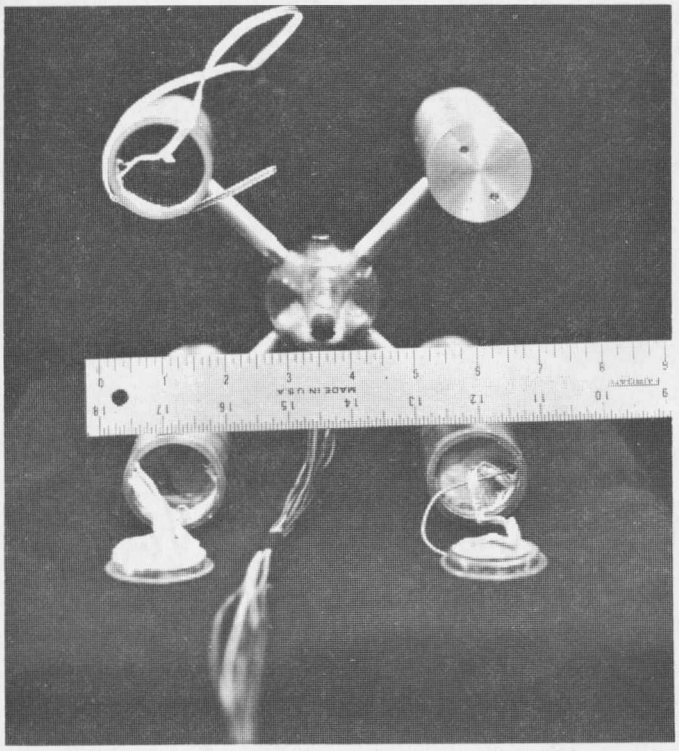


Figure 3.3 Inner Body Partially Assembled

minimize convection losses from all stainless steel tubing, the tubes were covered with a shrink tube having a low thermal conductivity. The support stem passed through the jacket walls of the bottom face of the outer body and was sealed with rubber O-rings.

A direct current power source and pressure sensitive heat tape provided the heating for the inner body. The heat tape, 0.064 cm thick and 0.32 cm wide, allowed for a maximum of 62 watts per foot under operating conditions of from 60 to 533 degrees K. The tape was applied to the entire inner surface of each tube and on the end caps utilizing two strips approximately 2.4 meters long with each starting at the midpoint of the tube and wrapped toward the end where it terminated by concentric wrapping on the end cap. Each end of the heat type was connected to power leads which were carried inside the support tubing. Since each half tube had separate power sources, it was possible to keep each cylinder isothermal when in the vertical position. Also, a high thermal conductivity copper material for the tubes was chosen to facilitate isothermality. Once the heat tapes were in place, they were coated with a silicone caulk which kept them securely in place and provided an insulated backing and the remainder of the tube opening was filled with fiberglass to ensure that convective currents would not induce an uneven temperature distribution on the tubes. Each of the eight heat tape input leads was connected to either a 2.0 or 0.5 amp ammeter (depending on the input power) then through variable power

resistors (35 ohm, 150 watt, 207 amp) and finally to the D.C. power sources. Voltages were read on a digital voltmeter connected through a multiple position switch to the low side of each variable resistor.

The temperature of each half tube was monitored by copper-constantan thermocouples epoxied into the wall of the tube approximately 0.025 cm from the outer surfaces. The two thermocouples per tube were placed on opposite sides of the cylinder at the one-quarter and three-quarter lengths. The entire system was assembled so that no two adjacent tubes had thermocouples in the same position. The leads to the thermocouples were passed through the support stem system and separately connected to a temperature reference source and digital millivoltmeter.

EXPERIMENTAL PROCEDURE

The following sequence outlines the procedure for acquisition of heat transfer data, temperature profiles, and visualization data. In each case the inner body was centered in the test chamber and the peripheral cooling system was activated. The cooling was monitored until the outer body became isothermal and equilibrium was established. Although equilibrium could be established within 6 to 8 hours, a longer time was allotted (24 hours) in order to fully test and check the seals on the inner chamber. When it was determined that the test chamber was operating satisfactorily, it was filled with a test fluid, and the

desired power (depending on fluid and desired temperature difference) was applied and adjusted to bring the inner body to isothermal equilibrium.

The heat transfer data points required the following measurements:

(1) Input voltage

(2) Input amperage

(3) Inner body temperature

(4) Outer body temperature

which were collected for each power setting. Utilizing 16 different fluid/geometry combinations, 166 data points were obtained. A listing of the fluids, body positions, and the partially reduced data is provided in Appendix II. Temperature profiles were always taken in conjunction with selected data runs. Each of the nine probes was positioned, in turn, against the inner body (reference position) and were withdrawn in increments ranging from 0.013 to 1.27 cm depending on the predicted temperature gradient. Position and thermocouple readings were recorded for 15 temperature profile sets. The above information was reduced by a computer program which converted thermocouple millivolt readings to K and calculated power input in watts. Visualization studies were conducted with air and the 20 cs fluid. Smoke, with air, and fluorescent paint particles mixed with the 20 cs fluid, provided the tracer particles needed for taking the photograph. The same procedures for the visualization apparatus were used as outlined in the

heat transfer data collection.

In order to minimize errors in data, several precautions were observed. All instrumentation was calibrated twice during the testing procedures. Once prior to initial testing of the body in the horizontal configuration and, finally, prior to tests in the vertical position. Power and cooling water controls were adjusted for each data run so that the variation in thermocouple readings in millivolts (TMVL) for the inner (I)(outer (O)) body met the following requirements:

$$\frac{TMVL_{I(O)_{max}} - TMVL_{I(O)_{min}}}{TMVL_{I_{min}} - TMVL_{O_{max}}} \approx 10\% \qquad (3.1)$$

The average variation in temperature for either the inner or outer body was within 4%, with a maximum variation of 15%.

The heat transferred by natural convection from the tubes was calculated by

$$Q_{CONV} = Q_{TOTAL} - Q_{RADIATION} - Q_{CONDUCTED} \quad . \qquad (3.2)$$

Of the four test fluids water, 99% glycerin, and the 20 cs fluid were opaque to radiation and the heat loss due to radiation was needed only for air. The procedure used to account for the heat loss due to the inner body support system proved to be complex and is, therefore, covered in a separate discussion provided in Appendix I. Only the discussion on radiation loss will be presented here. This procedure also accounts for conduction losses through the main support stem when

air is used as the working fluid.

The heat transferred by radiation was determined experimentally using the following procedure. The complete inner-outer body system was assembled and all thermocouple ports were plugged with solid wires. A vacuum pump was attached to the access tube which had been used to fill the test chamber with the test fluids and the chamber was evacuated to less than 10 microns. A minimum of 15 data points were collected over the range of ΔT's used in this study. These points were used in a least squares curve fit to develop an equation which could be used to correct all air data for radiation and conduction losses. The data points fit the equation with an average deviation of 1.49% and a maximum deviation of 3.73%. A second radiation calibration was made for the vertical configuration.

Having determined the heat transfer by natural convection from the four cylinders as indicated in equation (3.2), a final data reduction facilitated the development of correlating equations. The heat transfer (Q_{CONV}) allowed the computation of the average heat transfer coefficient (h) defined as follows:

$$h = \frac{Q_{CONV}}{A_c(T_I - T_O)} \qquad (3.3)$$

The fluid properties were calculated using the arithmetic mean temperature

$$T_{avg} = \frac{T_I + T_0}{2} \tag{3.4}$$

and the computer function subroutines listed in Appendix I of reference [14]. An exception to the above was the calculation of the properties of 99% glycerine which were taken from current literature. The specific heat for 100% glycerine was used as data for 99% was not available. As observed by Warrington [14], this did not affect the results.

CHAPTER IV

DISCUSSION OF RESULTS

Heat transfer results are discussed in terms of the dimensionless parameters defined in equations (2.2) through (2.4) and calculated from the data acquired from the procedures outlined in Chapter III. Further clarification must be made here since the Grashof and Nusselt numbers were calculated using two different characteristic dimensions. A hypothetical gap width which has been proven to be a reliable characteristic dimension in past investigations [14] was used and is defined as

$$L = R_o - R_i \tag{4.1}$$

where $R_o(R_i)$ is the radius of a sphere having the same volume as the outer(inner) body. Since the inner body was tested in two different orientations, a characteristic dimension based on the boundary layer length was defined for each. For the horizontal position of the cylinders, the boundary layer length was defined as

$$B = \frac{\pi}{2} \text{ (Diameter)} \tag{4.2}$$

and for the vertical position

$$B = \text{(Height + Diameter)} \tag{4.3}$$

with the assumption that for the Rayleigh number range involved in this study, there would be no separation of the boundary layer from the body. The ranges of these parameters are given in Table 4.1. Through flow

TABLE 4.1

RANGES OF THE DIMENSIONLESS PARAMETERS

FLUID	RANGE	Nu_L	Ra_L	Nu_B	Ra_B	Gr_L	Gr_B	Pr
AIR	MAX	21.18	$5.164X10^6$	33.50	$4.225X10^7$	$4.831X10^6$	$5.516X10^7$	0.7121
	MIN	7.889	$6.353X10^5$	10.57	$2.766X10^5$	$8.933X10^5$	$3.889X10^5$	0.7086
GLYCERIN	MAX	42.17	$1.021X10^8$	54.83	$3.748X10^8$	$1.936X10^5$	$3.419X10^5$	$3.13X10^4$
	MIN	10.28	$3.206X10^5$	6.353	$7.566X10^4$	$1.449X10^1$	3.427	$1.62X10^3$
WATER	MAX	65.02	$6.918X10^8$	114.8	$4.611X10^9$	$1.439X10^8$	$8.430X10^8$	10.45
	MIN	33.65	$3.639X10^7$	21.23	$8.586X10^6$	$3.828X10^6$	$9.053X10^5$	5.658
SILICONE	MAX	65.92	$6.887X10^8$	138.0	$5.173X10^9$	$5.508X10^6$	$3.697X10^7$	326.0
	MIN	37.50	$3.013X10^7$	23.23	$7.125X10^6$	$9.840X10^4$	$2.328X10^4$	187.3

visualization results this assumption was found to be accurate and will be discussed later. Reference to parameters which require a characteristic dimension will be subscripted L or B to denote the appropriate dimension.

Several equation forms were used to correlate the heat transfer data. The following four equation forms were found to consistently provide the best results and are used to present the results of this study:

$$Nu_x = C_1 \, Ra_x^{C_2} \quad , \tag{4.4}$$

$$Nu_x = C_1 \, Ra_x^{*C_2} \quad , \tag{4.5}$$

$$Nu_x = C_1 \, Ra_x^{C_2} \, Pr^{C_3} \quad , \tag{4.6}$$

$$Nu_x = C_1 \, Gr_x^{C_2} \, Pr^{C_3} \quad , \tag{4.7}$$

where the characteristic dimension (x) could be subscripted either L or B. Equation (4.5) is in terms of a modified Rayleigh number

$$Ra_x^* = Ra_x \cdot \frac{L}{R_i} \quad . \tag{4.8}$$

The constants C_1 through C_3 were determined by using a standard least squares curve fit.

Geometric effects were found to be significant and were generally consistent among the different fluids. The remainder of the discussion on results will be covered in the order of geometric effects, heat transfer results for each fluid, and heat transfer results for all data combined. Temperature profiles, flow visualizations, and comparisons with single body studies will be included in each section as they are applicable.

GEOMETRIC EFFECTS ON HEAT TRANSFER

When the inner body was changed from the horizontal to the vertical configuration there was a significant decrease in the heat transferred. This decrease was exhibited for all fluids, however, the relative magnitude varied for each fluid. The decrease in heat transfer between the two geometries is most pronounced in the low viscosity range (air) and becomes almost negligible in the high viscosity range (glycerine) as seen in Figure 4.1. The resulting decrease was 28%, 8%, 8%, and 2% for air, water, silicone, and glycerin, respectively, (in order of increasing Prandtl number). This suggests that the fluid viscosity tends to damp out geometric effects as was postulated by Weber [17]. However, Warrington [14] found no viscous effect on changing the diameter of a sphere in the enclosure. This is possibly because his geometric change was not as radical as that presented here.

The effects of the heat transferred by the lower cylinder on the

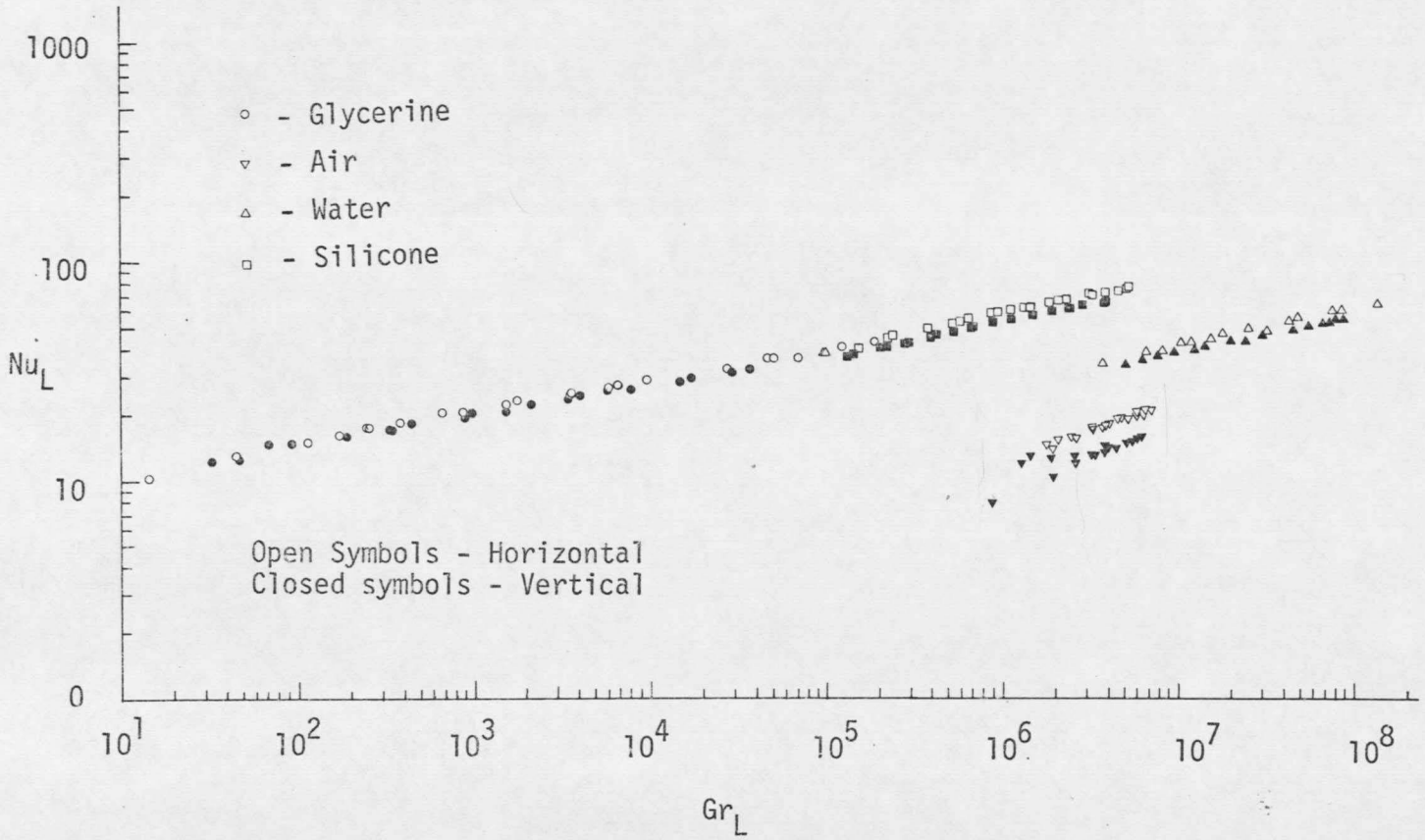


Figure 4.1 Nu_L versus Gr_L for All Data

upper cylinder in the horizontal position are similar to those observed by Eckert and Soehngen [8]. The lower cylinder preheated the fluid resulting in a reduced capacity of the fluid to transfer heat as the velocity field carried it around the upper cylinder. The reduced capacity for heat transfer in the fluid is a direct result of the lower ΔT or driving force for heat transfer. When the average Nusselt number for the upper cylinder was compared to the lower, the results were 84% of the bottom cylinder for air, 70% for glycerin, 89% for water, and 75% for silicone. Eckert and Soehngen [8] recorded 87% of the bottom cylinder using air with the distance between cylinders being four diameters. The results here are comparable and can be expected to show a stronger effect since a separation of only three diameters was used.

Since each half tube was separately heated, a similar analysis was available for the vertical position. The resulting average Nusselt number for the top half of each cylinder was 81% for air, 58% for glycerin, 64% for water, and 65% for silicone when compared to the bottom half. These results were expected since the length of the high speed flow along the body is long relative to the horizontal cylinder while the cross sectional flow area is much smaller. Thus the effect of the smaller driving force (ΔT) for heat transfer is more pronounced in the vertical configuration than in the horizontal. The evidence of a geometric effect is supported by both an overall decrease in heat transfer and a reduction in the average Nusselt number when upper and lower

halves of the inner body are compared.

A higher heat transfer from the horizontal cylinders as compared to the vertical cylinders results from the ability of the cooler medium to mix with the preheated fluid as it rises from the lower cylinder. Figures 4.2 through 4.8 show this effect. The major eddy, as seen in Figures 4.2 through 4.5, between the two cylinders, results from the mixing of cooler fluid into the flow. Figures 4.7 and 4.8 show that this eddy system for air is not as pronounced as for silicone. This may be a possible explanation for the larger decrease in the average Nusselt number (28%) as compared to the other fluids since the medium's cooling effect caused by the eddy is reduced. As the temperature of the cylinders is increased, another eddy is formed at the side of the upper cylinder indicating the same mixing action. This is evident in Figure 4.6. The introduction of cooler fluid from the sides and below was observed in other studies [9-11]. The eddy action as described was not evident in the vertical configuration, Figure 4.9. The flow visualizations in Figures 4.2 through 4.9 also support the assumption that the boundary layer does not separate from the cylinder with the exception of the top cap of the vertical cylinder. Correction in the boundary layer length for this separation had no effect on the deviation in fit for the correlating equations.

Two other geometries were studied. The inner body in both the vertical and horizontal orientations were rotated 45° about their

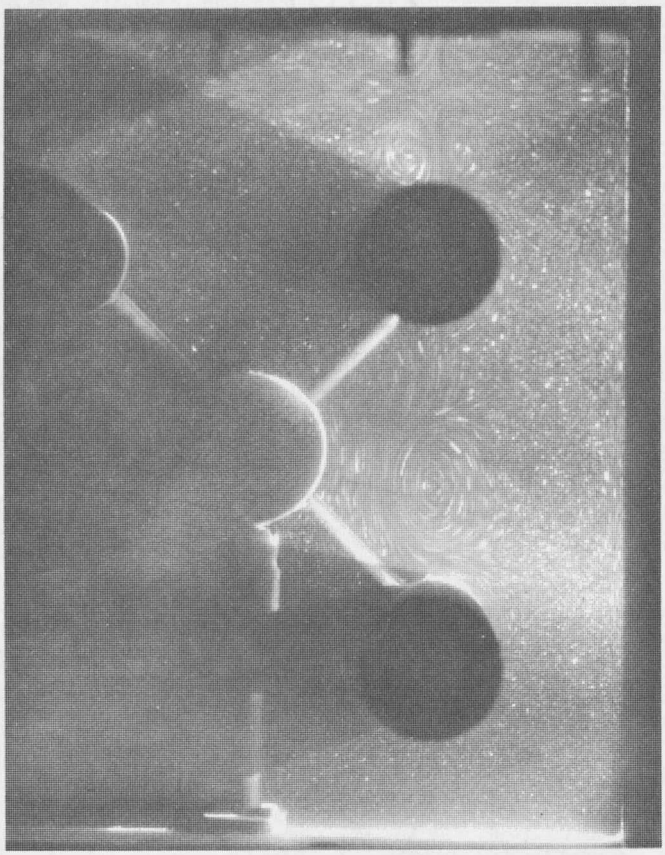


Figure 4.2 Flow Pattern for Horizontal Cylinders with 20 cs Fluid and ΔT = 10.71 K.

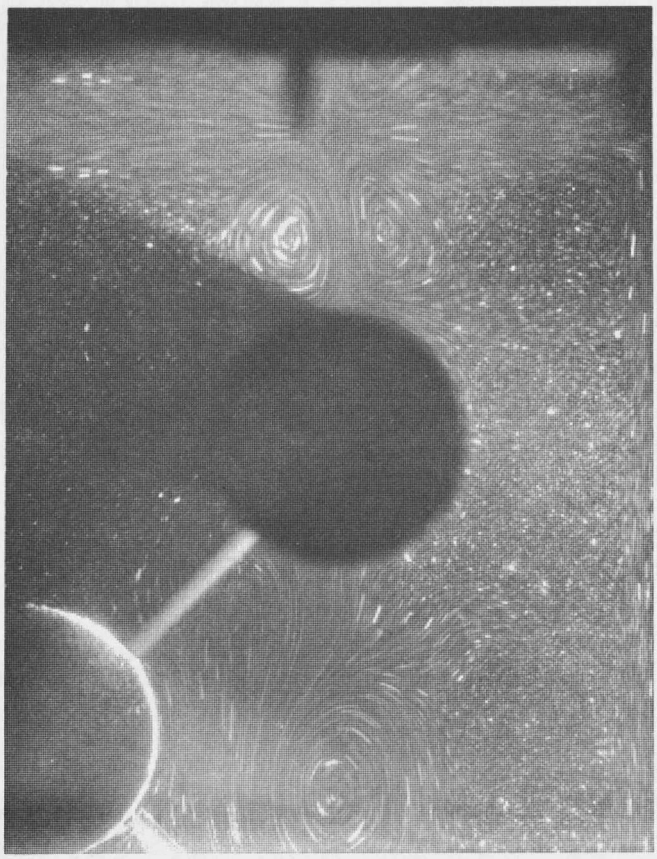


Figure 4.3 Flow Pattern Around Upper Horizontal Cylinder with 20 cs Fluid and ΔT = 10.71 K.

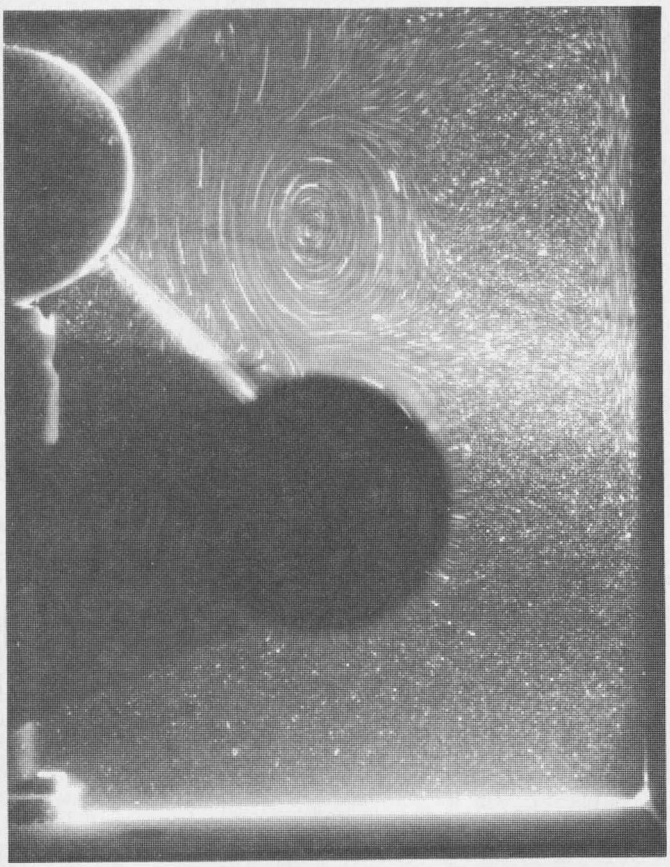


Figure 4.4 Flow Pattern Around Lower Horizontal Cylinder with 20 cs Fluid and ΔT = 10.71 K.

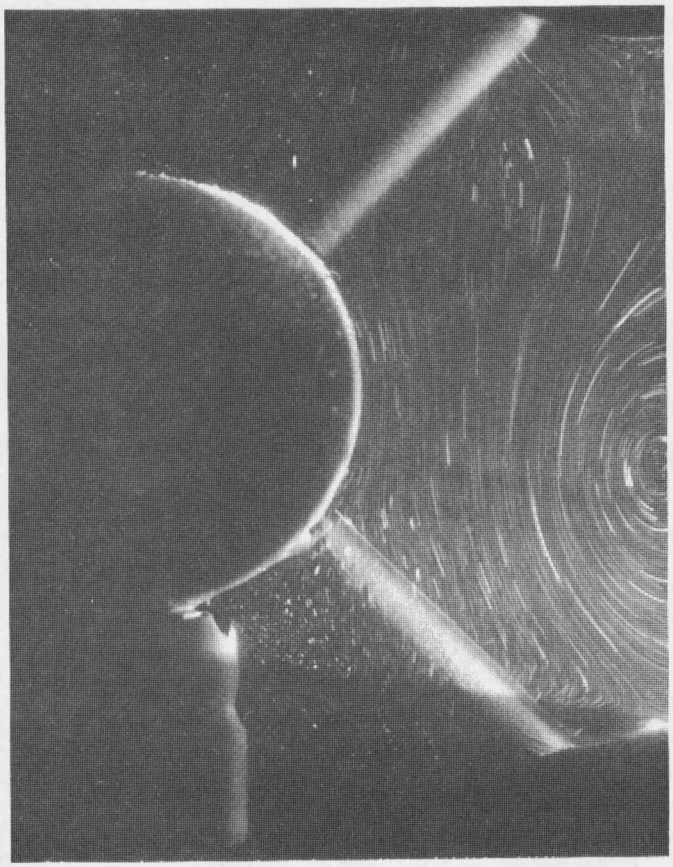


Figure 4.5 Flow Pattern Around Center Support Sphere with 20 cs Fluid and ΔT = 10.71 K.

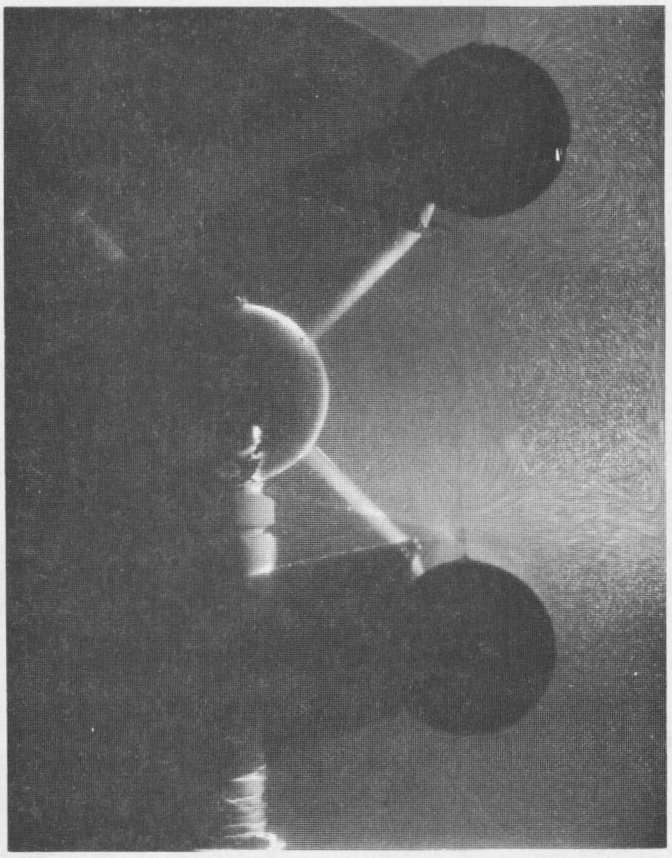


Figure 4.6 Flow Pattern for Horizontal Cylinders with 20 cs Fluid and ΔT = 54.43 K.

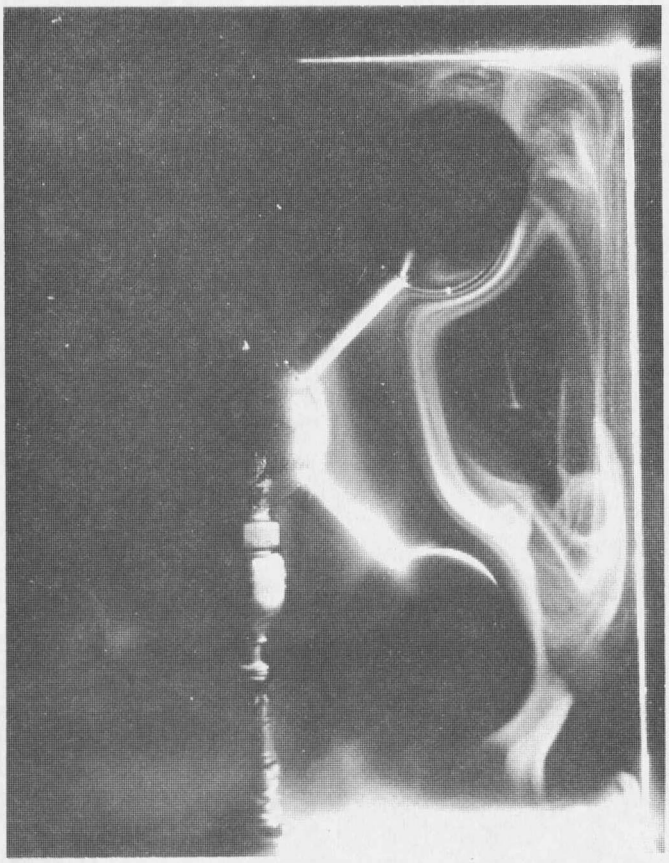


Figure 4.7 Flow Pattern for Horizontal Cylinders with Air and ΔT = 7.67 K.

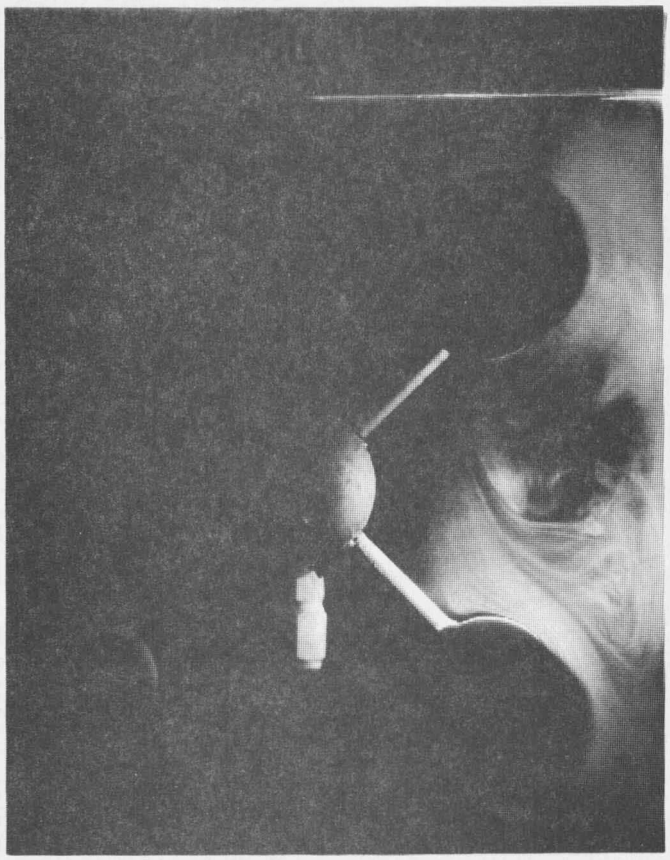


Figure 4.8 Flow Pattern for Horizontal Cylinders with Air and ΔT = 21.61 K.

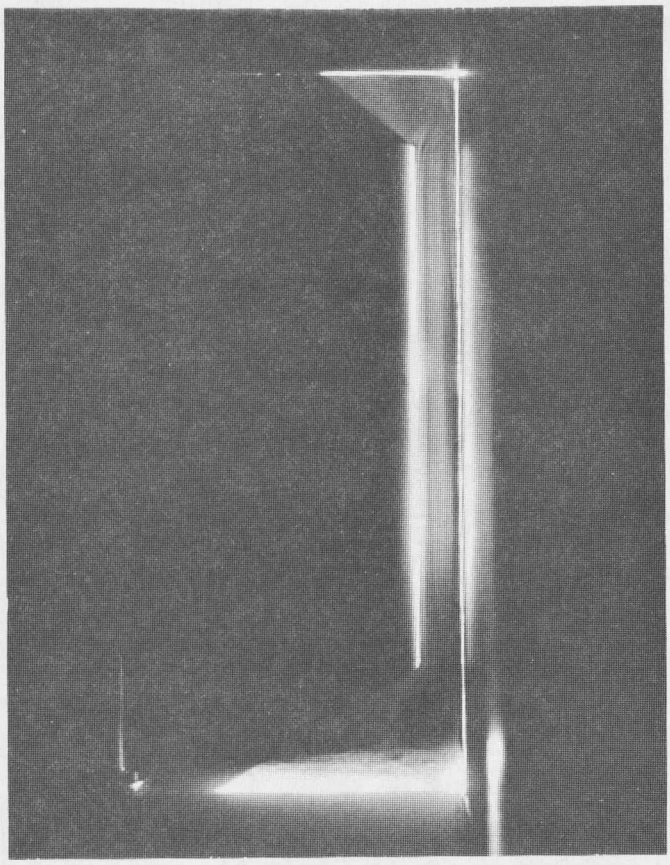


Figure 4.9 Flow Pattern for Vertical Cylinders with Air and ΔT = 17.01 K.

vertical axis. This rotation had negligible effect on the heat transfer. Utilizing the graphs of Nusselt number versus Grashof number for air, water, and the silicone fluid as shown in Figures 4.10 and 4.11, the 0° versus 45° rotation data points clearly indicate that this geometric change had negligible effect on the heat transfer results. Although the glycerin data are not presented, they exhibited the same pattern as the other fluids. The absence of any rotational effect was also evident in the temperature profiles. Figures 4.12 through 4.14 show show that for the same radial position the profiles for the 0° and 45° rotation do not change. These plots use dimensionless temperature and radius ratios and are defined as

$$T_{ND} = \frac{T - T_0}{T_I - T_0} \quad , \tag{4.9}$$

where T is the local temperature measured at any radial position and distance from the support sphere, and

$$R_{ND} = \frac{R}{R(\theta)} \quad , \tag{4.10}$$

where R is the local distance from the surface of the support sphere and $R(\theta)$ is the distance from the support sphere to the outer body depending on radial position. As seen in Figure 4.12 for the radial position $\theta = 120°$, a cylinder blocked the travel of a probe from reaching the support sphere and, therefore, the dimensionless distance could not

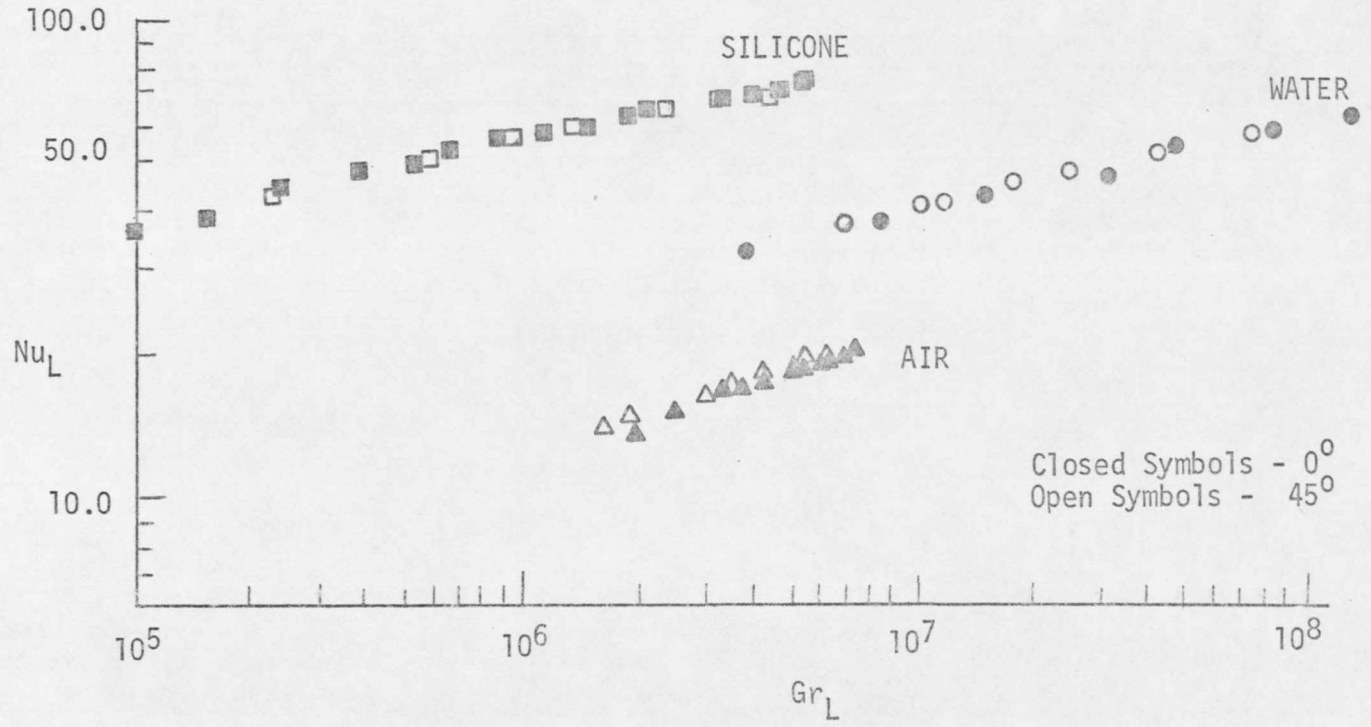


Figure 4.10 Nu_L versus Gr_L for 0^o and 45^o Rotations with the Cylinders in the Horizontal Position.

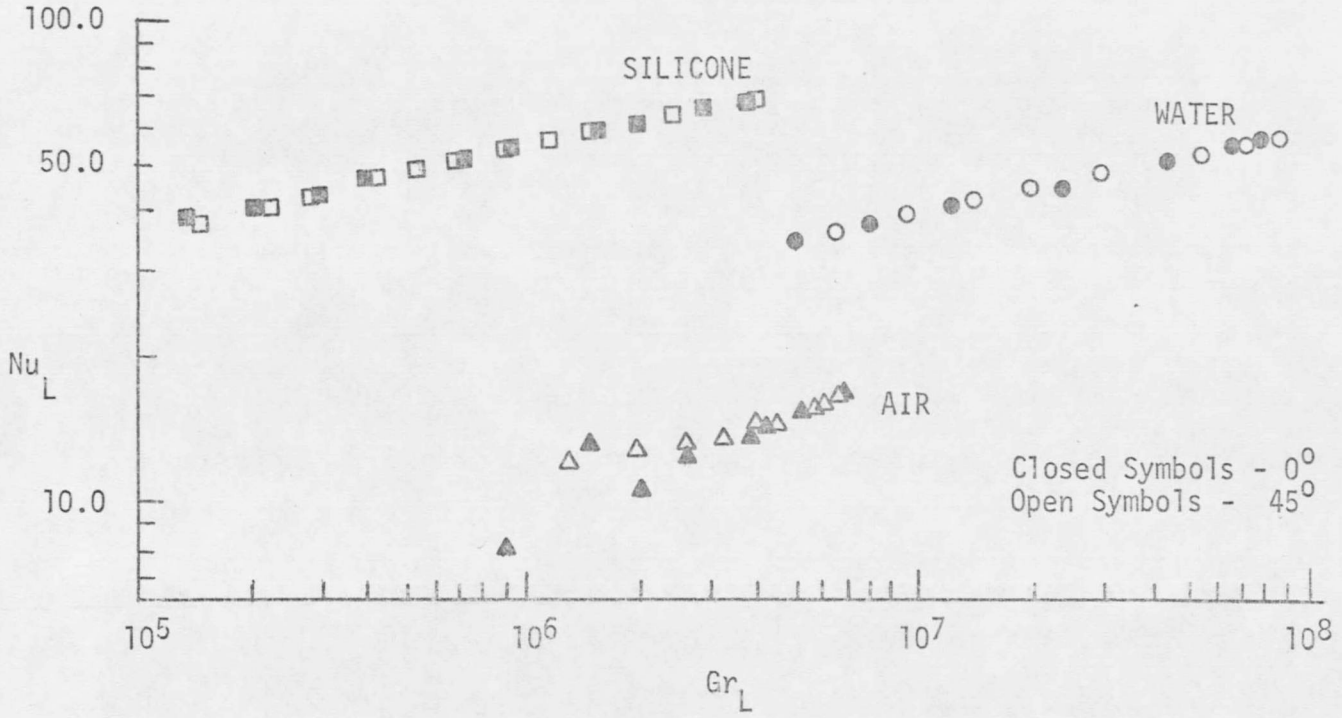


Figure 4.11 Nu_L versus Gr_L for 0^o and 45^o Rotations with the Cylinders in the Vertical Position.

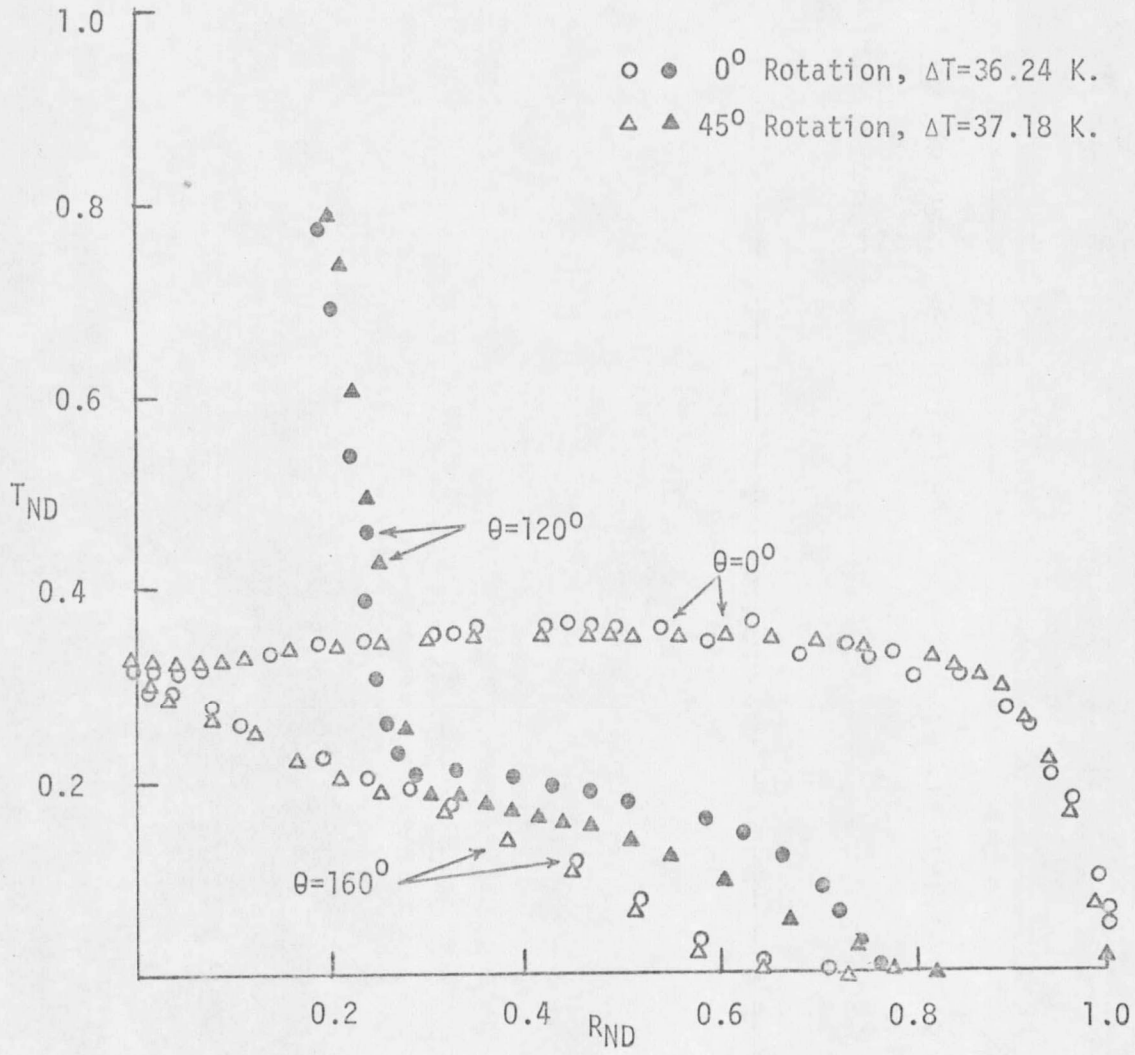


Figure 4.12 Temperature Profile for Rotation About the Vertical Axis with Silicone-Horizontal Position.

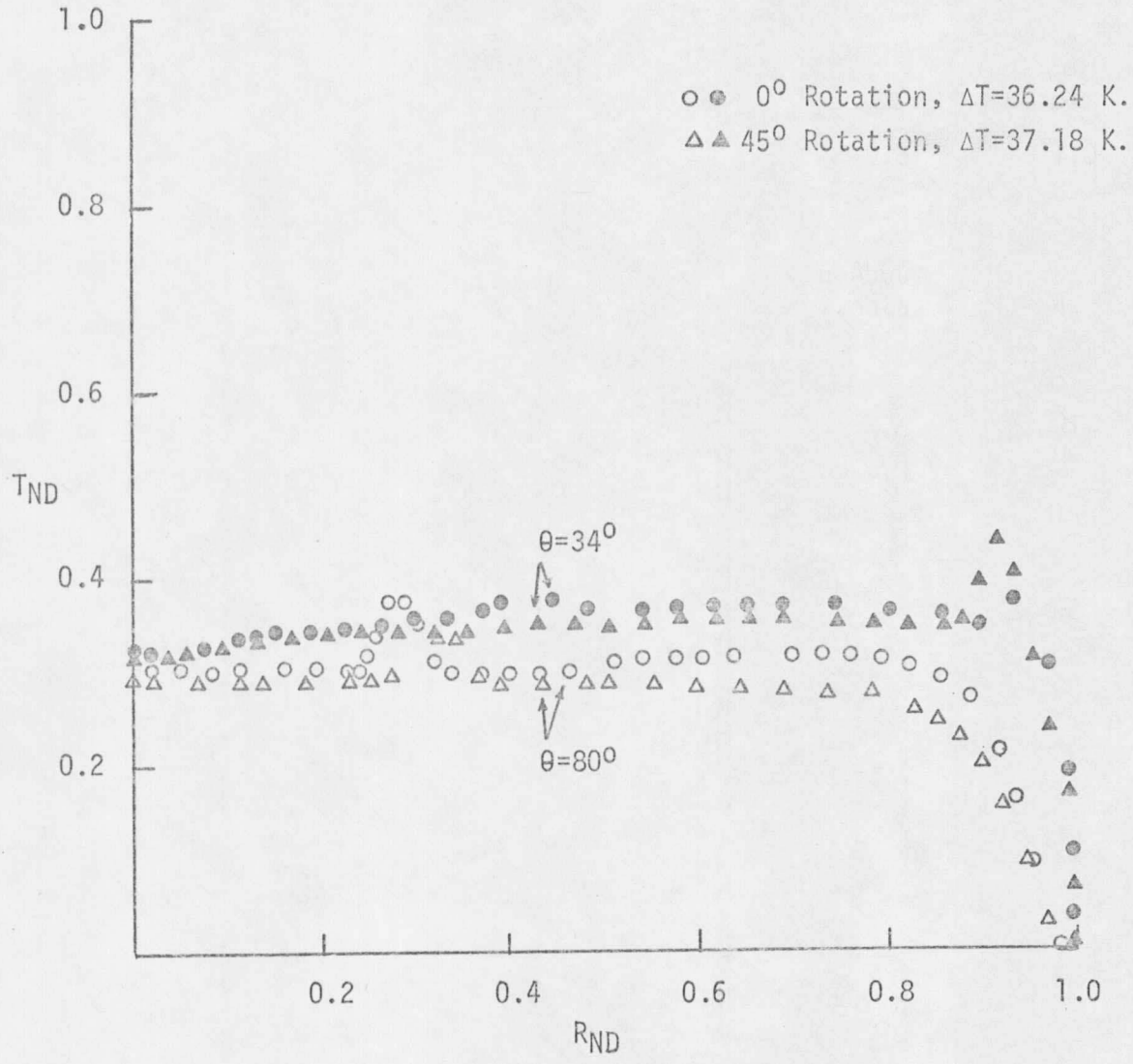


Figure 4.13 Temperature Profile for Rotation About the Vertical Axis with Silicone-Horizontal Position.

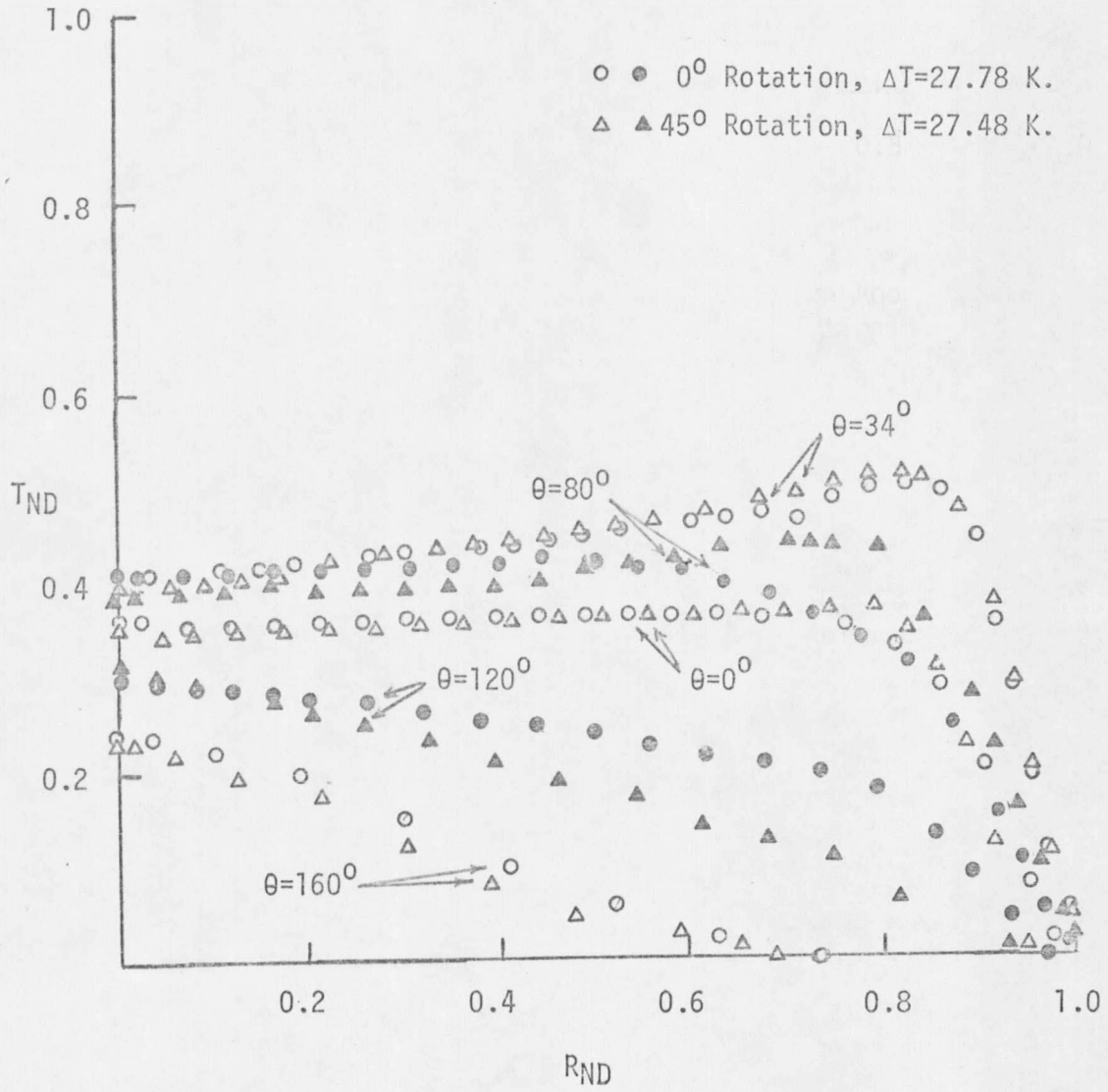


Figure 4.14 Temperature Profile for Rotation About the Vertical Axis with Glycerin-Vertical Position.

start at the zero reference point. All fluids exhibited the same effect as shown in Figures 4.12 through 4.14.

HEAT TRANSFER RESULTS USING AIR

The data using air as the fluid medium were correlated separately for both the horizontal and vertical geometries and also for all air data combined. Separate correlations for the rotational data (0° and 45°) are not presented since there was a negligible effect as previously described. The notation throughout the remainder of this discussion will consist of presenting a two-part designation in which the fluid will be given first, followed by the axial geometry; i.e., Air-Horizontal, Air-Vertical. When all data are presented the last term will be All. The scatter in the data for air, as seen in Figure 4.1, demonstrates the same pattern as described by Warrington [14]. The effect is pronounced in the lower temperature range which seems to support his conclusion that conduction and radiation losses may become a dominant factor as the fluid and molecular motion are reduced.

The best overall equation which correlates the heat transfer for the Air-Horizontal data was

$$Nu_L = 0.999\ Ra_L^{0.200} \qquad (4.11)$$

with an average percent deviation of 8.42 and maximum percent deviation of 18.70. Correlations using either the modified Rayleigh number

or the boundary length provided the same average deviations due to the constant geometry. The air data had the highest average deviation of all fluids. This can be directly attributed to the heat loss by radiation since all of the opaque fluids had a resulting average deviation approximately one magnitude smaller, as will be discussed later. The best correlation for Air-Vertical was

$$Nu_L = 0.293\ Ra_L^{0.260} \tag{4.12}$$

with 4.32% average deviation and 19.79% maximum deviation.

The best equation using a single correlation parameter for all air data was

$$Nu_B = 0.466\ Ra_B^{0.242} \tag{4.13}$$

with 6.79% average deviation. Correlations using the hypothetical gap width resulted in an average deviation of 16.48%. Compared to other fluids, air was affected the most by geometric orientation as shown in Figure 4.1 and its response to a correlation using the boundary layer length for the characteristic dimension as shown in Figure 4.15. Table 4.2 presents all correlations used for all air data combined. Equation forms (4.6) and (4.7) are not presented in the table since the set of equations generated by a least squares curve method form an ill-conditioned set when the Prandtl number is used as an independent parameter. This is a direct result of the very small variation in

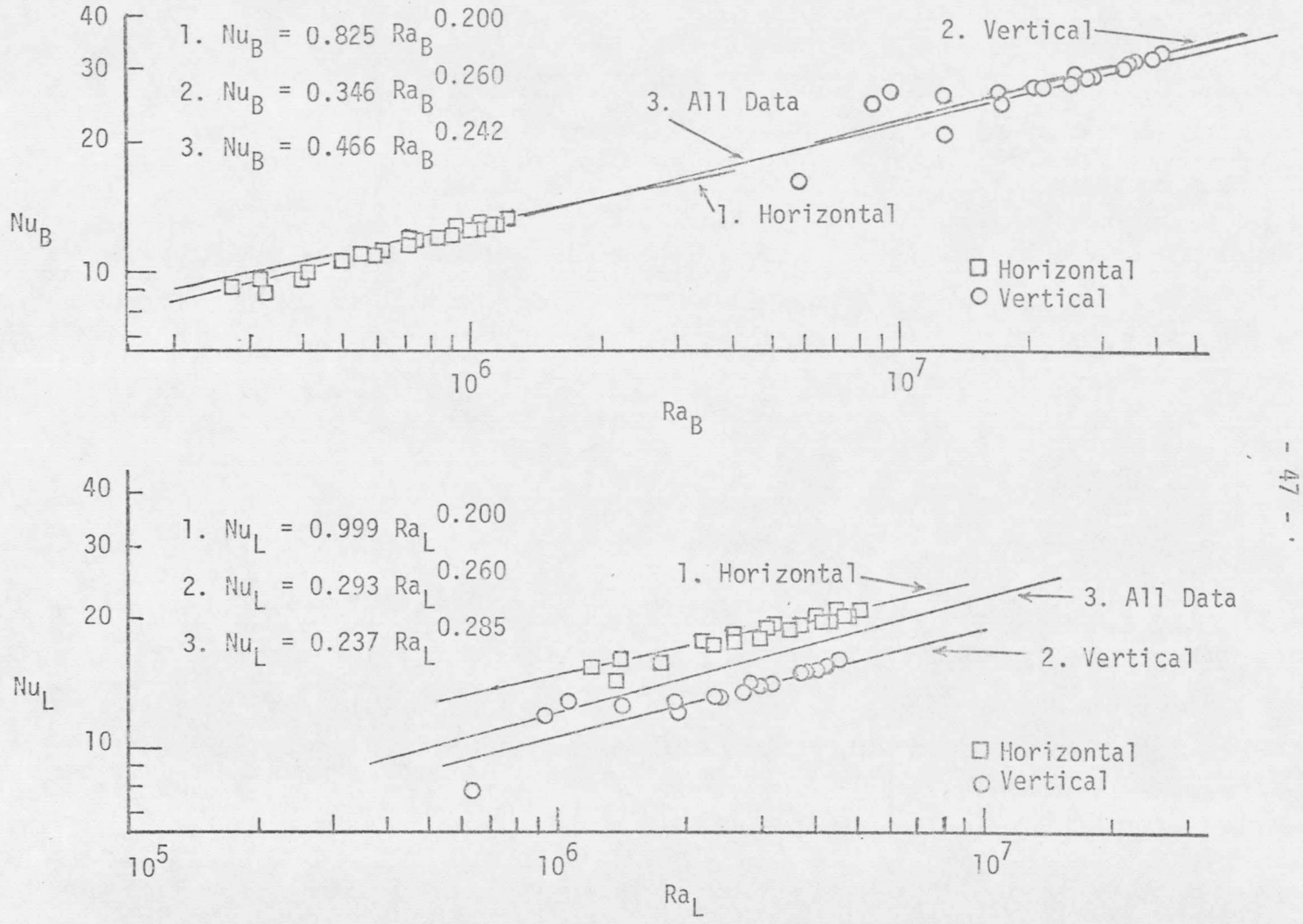


Figure 4.15 Nusselt Number versus Rayleigh Number for Air Data with Correlation Equations Superimposed.

TABLE 4.2

CORRELATION EQUATIONS FOR AIR-ALL

EQUATION	AVERAGE % DEVIATION	MAXIMUM % DEVIATION
$Nu_L = 0.237\ Ra_L^{0.285}$	16.487	36.212
$Nu_L = 0.203\ Ra_L^{*\ 0.285}$	16.487	36.212
$Nu_B = 0.466\ Ra_B^{0.242}$	6.795	22.626
$Nu_B = 0.409\ Ra_B^{*\ 0.242}$	6.795	22.626

Prandtl number for the air data. All air data have been plotted in Figure 4.15 in the form Nu_L versus Ra_L and Nu_B versus Ra_B with the best fit equations which used a single correlating parameter.

HEAT TRANSFER RESULTS USING GLYCERIN

Correlations using glycerin data provided very good results with average percent deviations ranging from 0.9% to 8.7% depending on the equation form used and the particular geometries involved. Using the gap width instead of boundary length as a correlating parameter affects only the coefficients and not the average deviation when applied to separate geometries. Therefore, only the equations using the gap width will be presented in the text. The tables will include the coefficients for equations using boundary layer length.

The best fit utilizing a single correlating parameter for Glycerin-Horizontal is

$$Nu_L = 0.547\ Ra_L^{0.236} \tag{4.14}$$

and for Glycerin-Vertical

$$Nu_L = 0.711\ Ra_L^{0.217} \tag{4.15}$$

with resulting average deviations of 1.72% and 0.913%, respectively. Correlations using two parameters improved the percent deviation only slightly as shown in Table 4.3.

TABLE 4.3

CORRELATIONS FOR GLYCERIN DATA

Equation Form	Glycerin-Horizontal			Glycerin-Vertical			Glycerin-All		
	C_1	C_2	C_3	C_1	C_2	C_3	C_1	C_2	C_3
	Avg % Deviation		Max % Deviation	Avg % Deviation		Max % Deviation	Avg % Deviation		Max % Deviation
$Nu_L = C_1 Ra_L^{C_2}$	0.548	0.236	———	0.711	0.217	———	0.595	0.230	———
	1.722		6.216	0.912		6.589	2.624		7.246
$Nu_L = C_1 Ra_L^{*C_2}$	0.482	0.236	———	0.633	0.217	———	0.525	0.230	———
	1.722		6.216	0.913		6.589	2.624		7.246
$Nu_L = C_1 Ra_L^{C_2} Pr^{C_3}$	0.096	0.299	0.094	3.454	0.162	-0.086	1.511	0.197	-0.050
	1.638		4.457	1.150		5.070	2.540		7.557
$Nu_B = C_1 Ra_B^{C_2}$	0.476	0.236	———	0.918	0.217	———	0.244	0.287	———
	1.722		6.216	0.913		6.589	8.714		24.88
$Nu_B = C_1 Ra^{*C_2}$	0.419	0.236	———	0.818	0.217	———	0.209	0.287	———
	1.722		6.216	0.913		6.589	8.714		24.89
$Nu_B = C_1 Ra_B^{C_2} Pr^{C_3}$	0.092	0.298	0.094	5.066	0.162	-0.086	0.045	0.321	0.139
	1.638		4.457	1.150		5.071	1.757		11.67
$Nu_L = C_1 Gr_L^{C_2} Pr^{C_3}$	0.096	0.298	0.392	3.454	0.162	0.076	1.511	0.197	0.146
	1.638		4.457	1.150		5.070	2.539		7.557
$Nu_B = C_1 Gr_B^{C_2} Pr^{C_3}$	0.135	0.298	0.392	5.066	0.162	0.076	0.045	0.321	0.461
	1.638		4.457	1.150		5.071	1.757		11.67

Correlations of all glycerin data was best accomplished using the hypothetical gap width rather than the boundary layer when using one parameter. As discussed previously, the glycerin data were affected very little by the geometry as a result of the dampening effects of viscosity. The use of the boundary layer length as a characteristic dimension over-predicts the geometric effects causing the correlations based on this dimension to yield a higher average percent deviation. Figure 4.16 reveals this over-prediction through a shift in the vertical data as seen in the graph of Nu_B versus Ra_B. Both water and silicone were affected in the same manner although to a lesser degree.

The correlations which provided the best results for all glycerin data were

$$Nu_L = 0.595\ Ra_L^{0.230} \tag{4.16}$$

and

$$Nu_L = 1.511\ Ra_L^{0.197}\ Pr^{-0.050} \tag{4.17}$$

with respective average deviations of 2.62% and 2.54%. Figure 4.16 provides a plot of Nu versus Ra and the single parameter correlation equations.

HEAT TRANSFER DATA USING WATER AND SILICONE

Water and silicone exhibited similar heat transfer results and

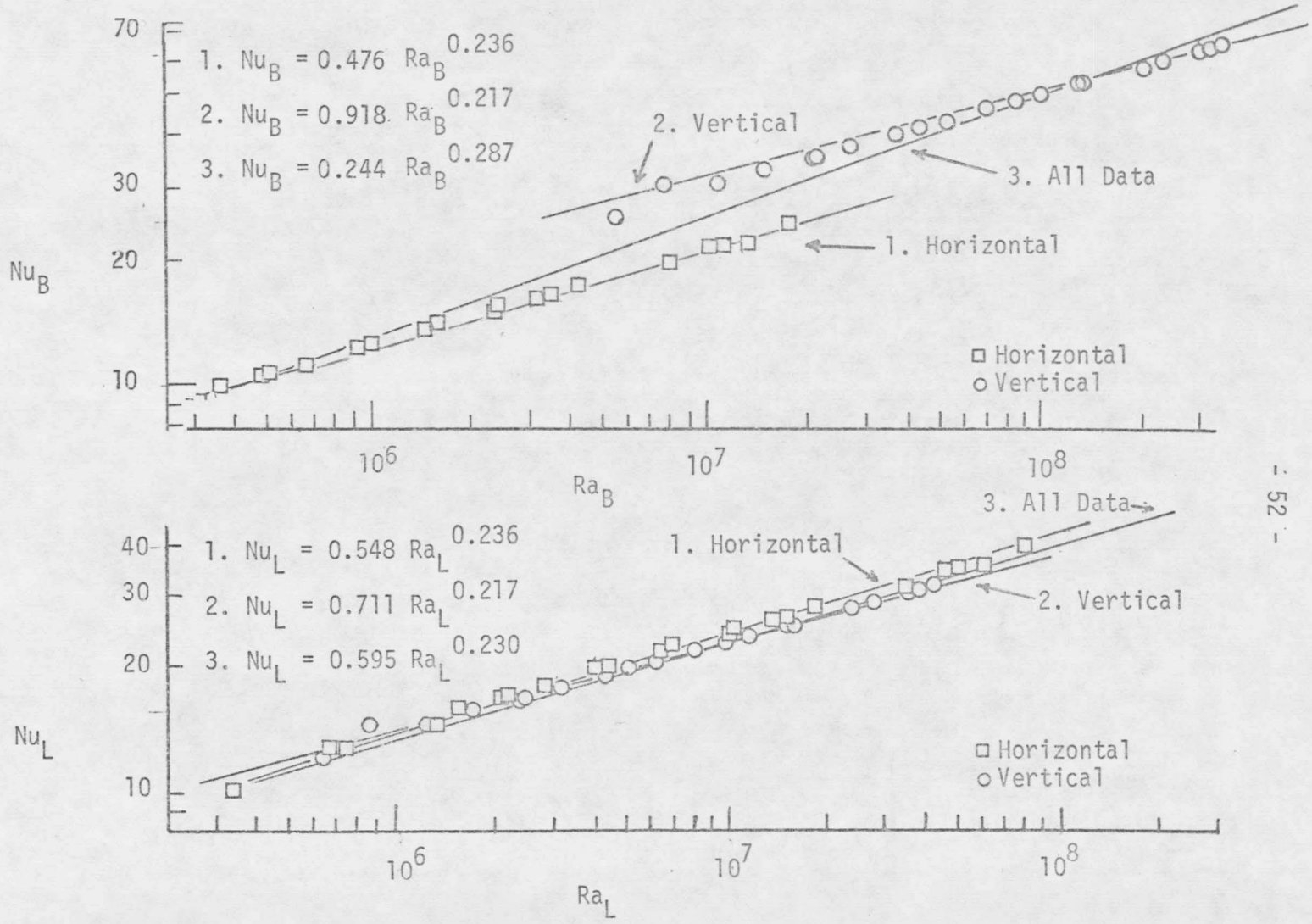


Figure 4.16 Nusselt Number versus Rayleigh Number for Glycerin Data with Correlation Equations Superimposed.

are combined into one section. Correlations for both fluids yielded average deviations which ranged from 1.26% to 6.16%. These results as well as those for glycerin all indicate that correlations for a single fluid can be expected to yield satisfactory results.

Table 4.4 presents all equations and geometries for the correlation of water data. Correlations which provided the best fit of data using one and two parameters for all water data are

$$Nu_L = 0.888\ Ra_L^{0.208} \tag{4.18}$$

and

$$Nu_B = 0.053\ Ra_B^{0.310} Pr^{0.463} \tag{4.19}$$

with average deviations of 4.40% and 1.97%, respectively. Figure 4.17 presents all water data and the best fit equation in graphical form.

The data for silicone is presented in Figure 4.18 and the resulting correlations are presented in Table 4.5. Best fit equations for the silicone fluid using one and two parameters are

$$Nu_L = 0.709\ Ra_L^{0.228} \tag{4.20}$$

and

$$Nu_B = 0.035\ Ra_B^{0.308} Pr^{0.284} \tag{4.21}$$

with average deviations of 4.28% and 1.26%, respectively.

TABLE 4.4

CORRELATIONS FOR WATER DATA

Equation Form	Water-Horizontal			Water-Vertical			Water-All		
	C_1	C_2	C_3	C_1	C_2	C_3	C_1	C_2	C_3
	Avg % Deviation		Max % Deviation	Avg % Deviation		Max % Deviation	Avg % Deviation		Max % Deviation
$Nu_L = C_1 Ra_L^{C_2}$	0.783	0.217	———	1.020	0.199	———	0.888	0.208	———
	1.286		5.069	.563		2.292	4.401		8.013
$Nu_L = C_1 Ra_L^{*C_2}$	0.696	0.217	———	0.917	0.199	———	0.793	0.208	———
	1.286		5.069	.563		2.292	4.401		8.013
$Nu_L = C_1 Ra_L^{C_2} Pr^{C_3}$	1.277	0.200	-.080	1.580	0.183	-0.076	0.318	0.244	0.172
	1.240		5.080	0.540		2.291	4.277		8.133
$Nu_B = C_1 Ra_B^{C_2}$	0.661	0.217	———	1.379	0.199	———	0.180	0.293	———
	1.286		5.0692	0.563		2.292	6.170		14.27
$Nu_B = C_1 Ra^{*C_2}$	0.588	0.217	———	1.235	0.199	———	0.154	0.293	———
	1.286		5.069	0.563		2.292	6.170		14.27
$Nu_B = C_1 Ra_B^{C_2} Pr^{C_3}$	1.055	0.200	-0.080	2.226	0.183	-.076	0.053	0.310	0.463
	1.240		5.080	0.540		2.291	1.970		4.973
$Nu_L = C_1 Gr_L^{C_2} Pr^{C_3}$	1.277	0.200	0.120	1.580	0.183	0.107	0.318	0.244	0.4170
	1.240		5.080	0.540		2.291	4.277		8.133
$Nu_B = C_1 Gr_B^{C_2} Pr^{C_3}$	1.055	0.200	0.120	2.226	0.183	0.107	0.053	0.310	0.773
	1.240		5.080	0.540		2.291	1.970		4.973

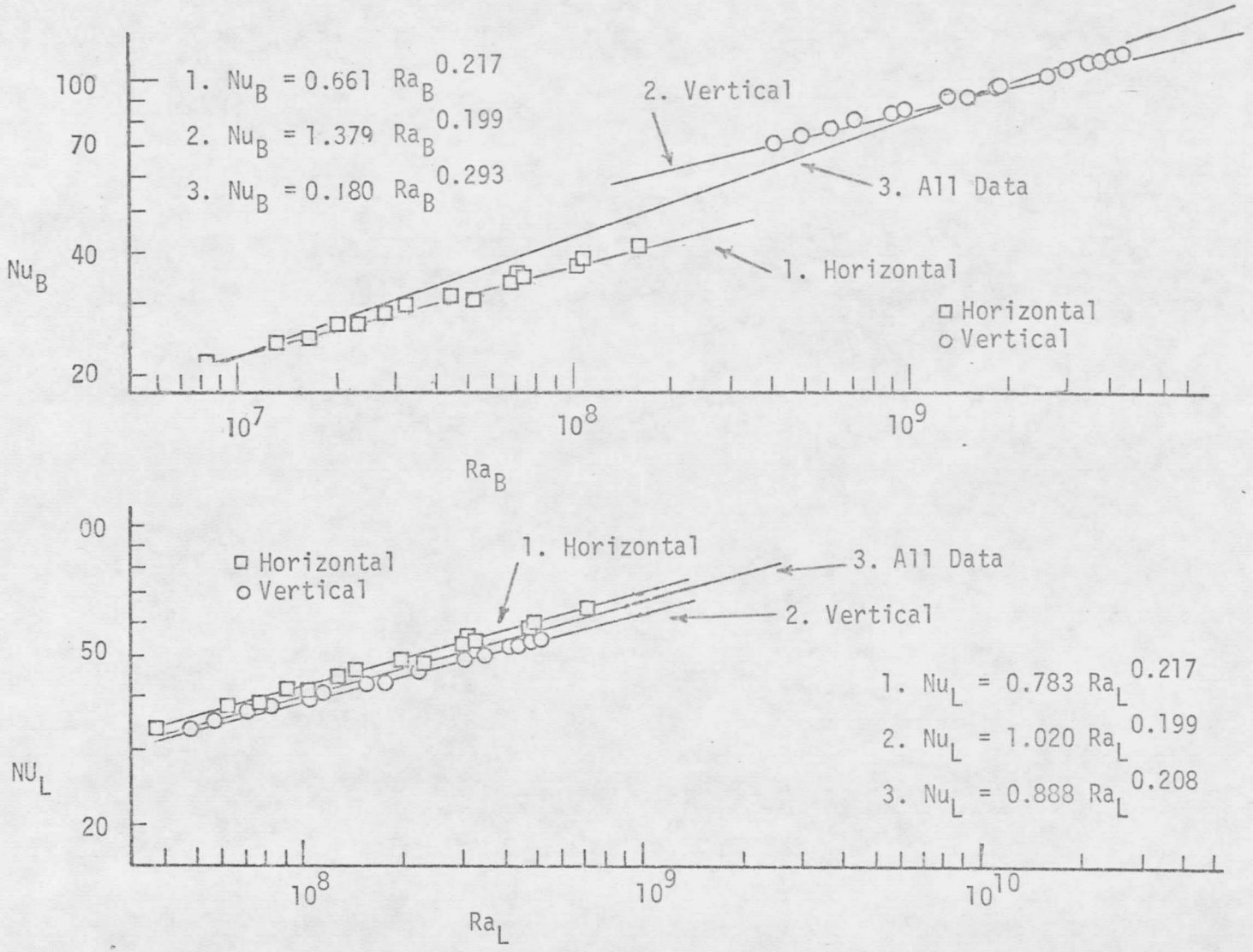


Figure 4.17 Nusselt Number versus Rayleigh Number for Water Data with Correlation Equations Superimposed.

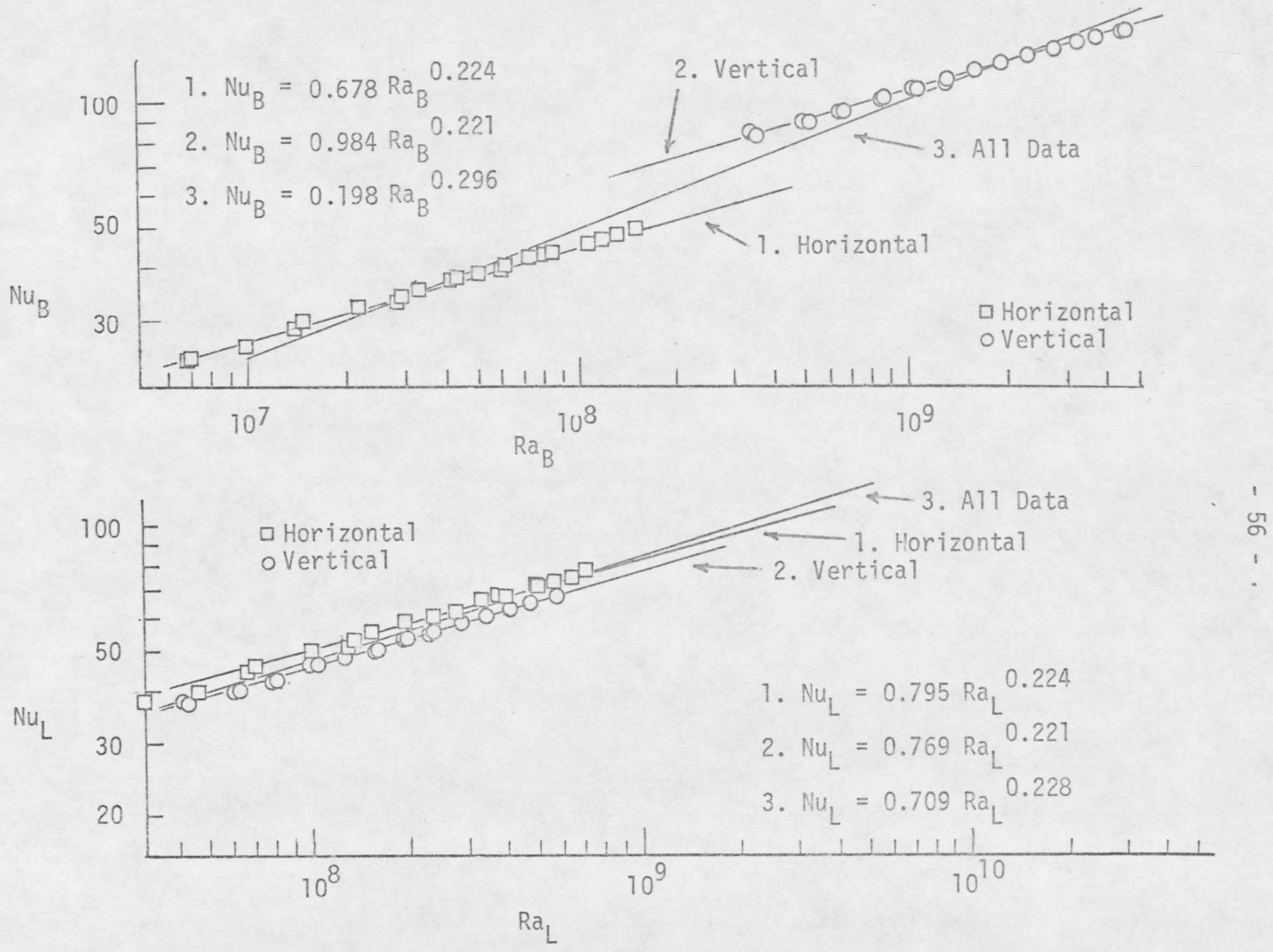


Figure 4.18 Nusselt Number versus Rayleigh Number for Silicone Data with Correlation Equations Superimposed.

TABLE 4.5

CORRELATIONS FOR SILICONE DATA

Equation Form	Silicone-Horizontal			Silicone-Vertical			Silicone-All		
	C_1	C_2	C_3	C_1	C_2	C_3	C_1	C_2	C_3
	Avg % Deviation	Max % Deviation		Avg % Deviation	Max % Deviation		Avg % Deviation	Max % Deviation	
$Nu_L = C_1 Ra_L^{C_2}$	0.795	0.224	———	0.769	0.221	———	0.709	0.228	———
	0.888	2.985		0.607	2.867		4.284	6.818	
$Nu_L = C_1 Ra_L^{*C_2}$	0.703	0.224	———	0.683	0.221	———	0.627	0.228	———
	0.888	2.985		0.607	2.867		4.284	6.818	
$Nu_L = C_1 Ra_L^{C_2} Pr^{C_3}$	0.404	0.242	0.062	0.681	0.224	0.011	1.864	0.202	-0.090
	0.815	2.672		0.602	2.948		4.196	7.013	
$Nu_B = C_1 Ra_B^{C_2}$	0.678	0.224	———	0.984	0.221	———	0.198	0.296	———
	.888	2.985		0.607	2.867		5.912	15.14	
$Nu_B = C_1 Ra^{*C_2}$	0.600	0.244	———	0.873	0.221	———	0.167	0.296	———
	.888	2.985		0.607	2.867		5.912	15.14	
$Nu_B = C_1 Ra_B^{C_2} Pr^{C_3}$	0.354	0.242	0.062	0.868	0.225	0.114	0.035	0.308	0.284
	.815	2.672		0.602	2.948		1.256	5.892	
$Nu_L = C_1 Gr_L^{C_2} Pr^{C_3}$	0.404	0.242	0.305	0.681	0.225	0.236	1.864	0.202	0.113
	0.815	2.672		0.602	2.948		4.196	7.013	
$Nu_B = C_1 Gr_B^{C_2} Pr^{C_3}$	0.354	0.242	0.305	0.868	0.225	0.236	0.035	0.308	0.591
	0.815	2.672		0.602	2.948		1.256	5.892	

Results concerning the effects of geometry and fluid properties have generally the same characteristics as the results for glycerin. These relationships between fluids and geometries are covered in the next section.

HEAT TRANSFER RESULTS FOR ALL FLUIDS

In addition to the correlations already discussed, three other combinations of data were correlated. Data for all fluids were correlated against horizontal, vertical, and both geometries. The resulting decrease in the accuracy of all equation forms, when compared to the single fluid correlations, can be directly associated with the Prandtl number effect. This is evident in Table 4.6 and Figure 4.1.

Table 4.6 includes all correlation equation forms using data combinations described above. The best fit for all data, all vertical data and all horizontal data using the gap width are

$$Nu_L = 0.358\ Ra_L^{0.257} Pr^{0.014} \quad , \tag{4.22}$$

$$Nu_L = 0.262\ Ra_L^{0.268} Pr^{0.028} \quad , \tag{4.23}$$

and

$$Nu_L = 0.498\ Ra_L^{0.245} Pr^{-0.002} \quad , \tag{4.24}$$

with average deviations of 8.38%, 4.53%, and 6.92%, and maximum deviations of 40.45%, 18.48%, and 14.74%, respectively.

TABLE 4.6

CORRELATIONS FOR ALL DATA

Equation Form	All-Horizontal			All-Vertical			All Data		
	C_1	C_2	C_3	C_1	C_2	C_3	C_1	C_2	C_3
	Avg % Deviation		Max % Deviation	Avg % Deviation		Max % Deviation	Avg % Deviation		Max % Deviation
$Nu_L = C_1 Ra_L^{C_2}$	0.496	0.245	———	0.264	0.274	———	0.365	0.259	———
	6.947		15.27	9.340		30.58	9.500		47.71
$Nu_L = C_1 Ra_L^{*C_2}$	0.435	0.245	———	0.227	0.274	———	0.317	0.259	———
	6.947		15.27	9.340		30.58	9.500		47.71
$Nu_L = C_1 Ra_L^{C_2} Pr^{C_3}$	0.498	0.245	-0.002	0.262	0.268	0.028	0.358	0.257	0.014
	6.916		14.74	4.531		18.48	8.384		40.453
$Nu_B = C_1 Ra_B^{C_2}$	0.437	0.245	———	0.300	0.274	———	0.286	0.275	———
	6.947		15.27	9.340		30.58	9.305		28.63
$Nu_B = C_1 Ra^{*C_2}$	0.383	0.245	———	0,259	0.274	———	0.246	0.275	———
	6.947		15.27	9.340		30.58	9.305		28.63
$Nu_B = C_1 Ra_B^{C_2} Pr^{C_3}$	0.438	0.245	-0.002	0.302	0.268	0.028	0.277	0.274	0.012
	6.916		14.74	4.531		18.48	8.437		24.85
$Nu_L = C_1 Gr_L^{C_2} Pr^{C_3}$	0.498	0.245	0.244	0.262	0.268	0.297	0.358	0.257	0.271
	6.916		14.74	4.531		18.48	8.384		40.45
$Nu_B = C_1 Gr_B^{C_2} Pr^{C_3}$	0.438	0.245	0.243	0.302	0.268	0.297	0.277	0.274	0.286
	6.916		14.74	4.531		18.48	8.437		24.85

As mentioned previously, the correlations for single geometries were not affected by the change from one characteristic dimension to another. Correlation of all data indicated an appreciable improvement when the boundary layer length was used, resulting in an 8.44% average deviation and 24.85% maximum deviation versus 8.38% and 40.45%, respectively, for correlations using the gap width. The best equation for all data was

$$Nu_B = 0.277\ Ra_B^{0.274} Pr^{0.012} \quad . \tag{4.25}$$

The relatively small value of the exponent associated with the Prandtl number suggests that this term can be dropped without appreciable loss in accuracy. The resulting equation

$$Nu_B = 0.286\ Ra_B^{0.275} \tag{4.26}$$

has a 9.30% average deviation and 28.63% maximum deviation. Figures 4.19 and 4.20 provide a plot of all data against the best fit equations using a single correlating parameter.

Warrington [14] provides one of the most exhaustive studies in heat transfer in enclosures to date. In correlating several single body geometries, fluids and outer body geometries, he found that the best single parameter equation using the gap width was

$$Nu_L = 0.181\ Ra_L^{*0.282} \tag{4.27}$$

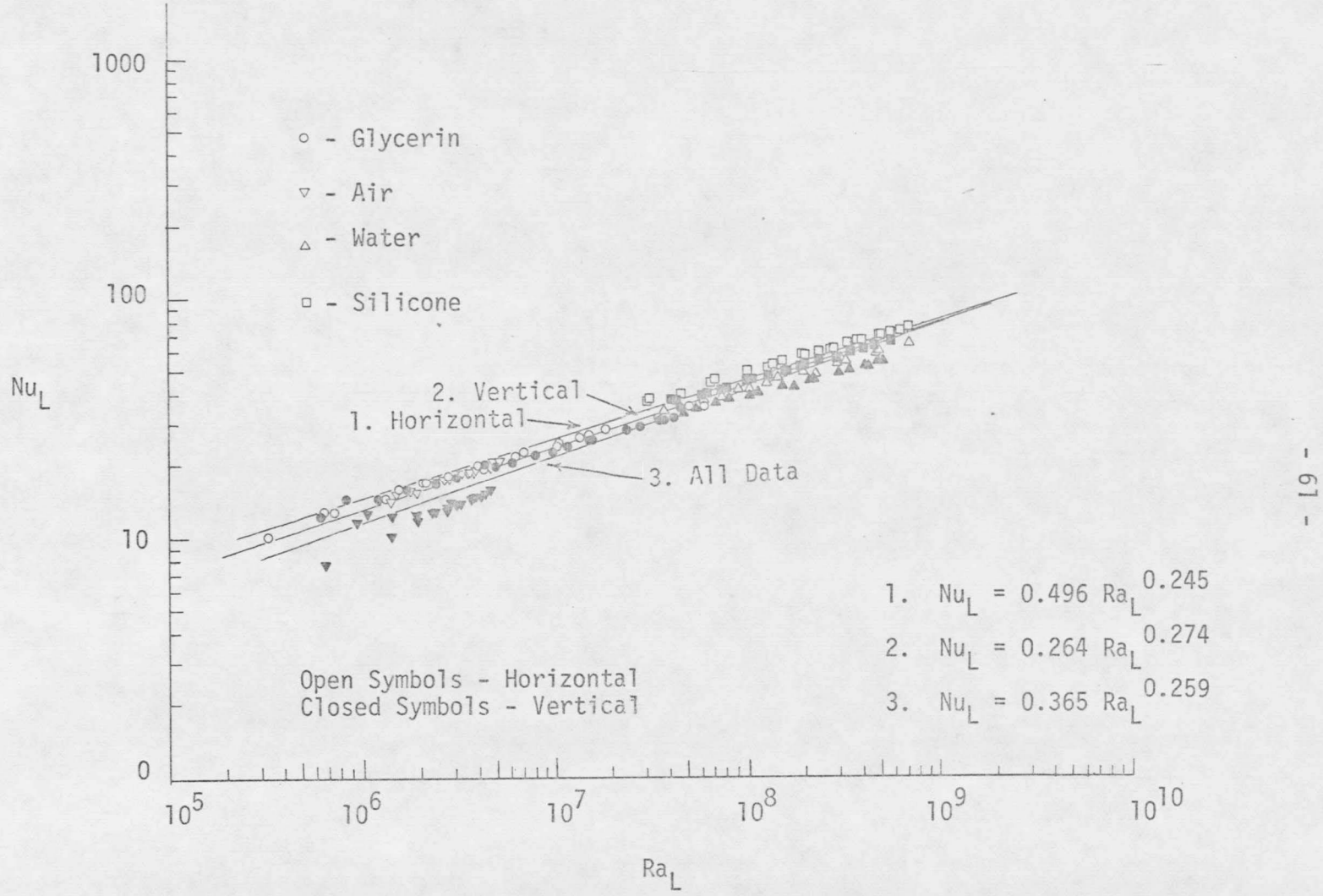


Figure 4.19 Nu_L versus Ra_L for All Data with Correlation Equations Superimposed

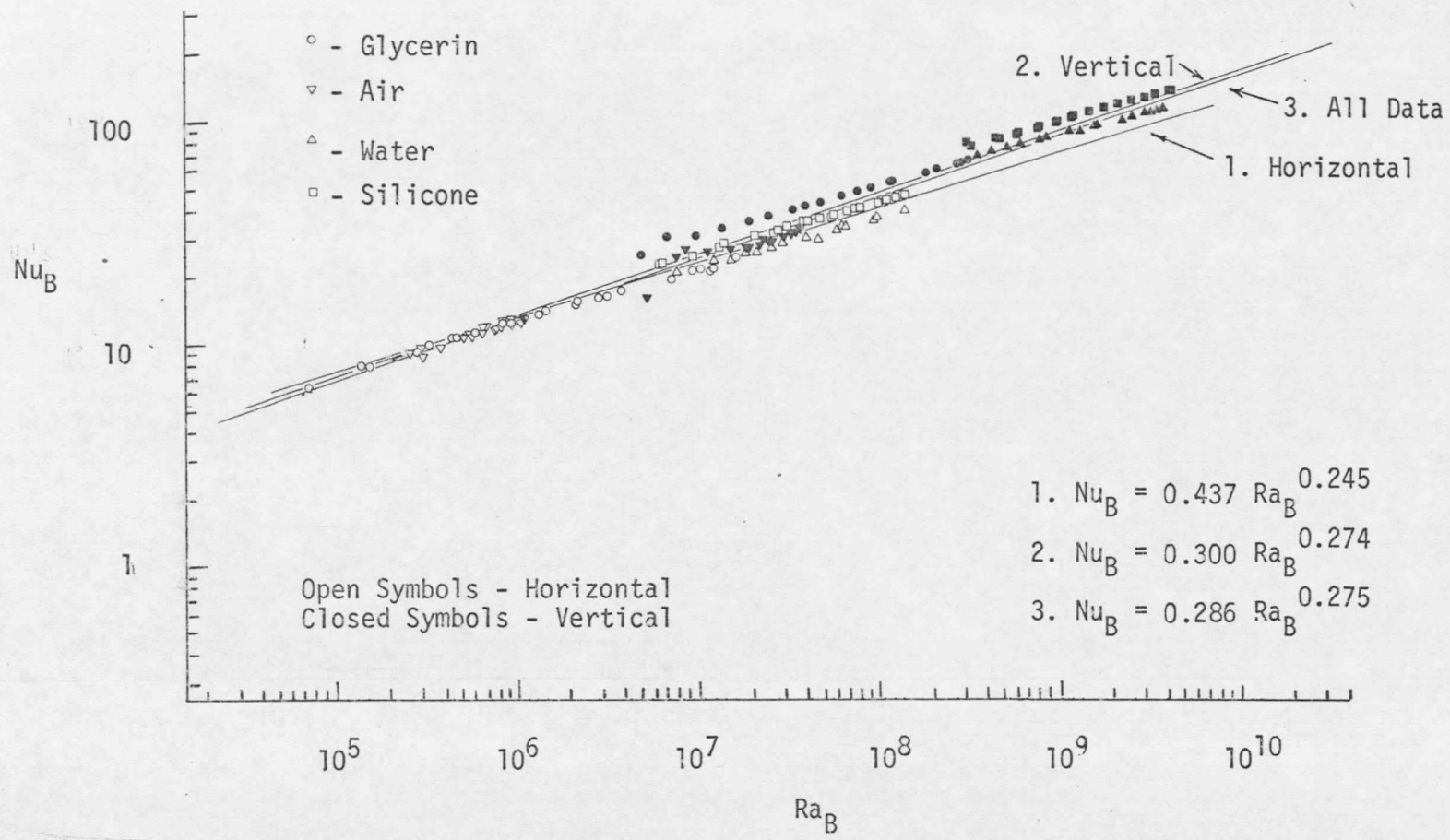


Figure 4.20 Nu_B versus Ra_B for All Data with Correlation Equations Superimposed

with an 18.67 average percent deviation, and the best fit using the boundary layer length was

$$Nu_B = 0.585\ Ra_B^{*0.236} \tag{4.28}$$

with a 14.75% average deviation. The data encompassed by this investigation were correlated with the above equations and resulted in 13.04% and 20.34% average deviations, respectively. However, this required a redefinition of the boundary layer length to include the total boundary length for all four cylinders. Correlations using the boundary layer length for one cylinder as used in this study provided unacceptable results when applied to the equations for single bodies which have been developed by Warrington. These equations with current data fitted to them are provided in Table 4.7. Even with a redefined boundary layer length, the relatively large deviation from equation (4.28) and the slightly larger differences as seen in Table 4.7 for correlations using the boundary layer dimension, suggest that the heat transfer is complicated by the multiple body geometry and the tendency to over-predict these geometric effects as previously discussed.

TABLE 4.7

FIT OF DATA TO PREVIOUSLY DEVELOPED EQUATIONS

The following equations were extracted from reference [14]:

EQUATION	AVG % DEV.	CONDITIONS FOR USE
1. $Nu_B = 0.585\ Ra_B^{*0.236}$	14.75	Single inner bodies (cube, sphere, and cylinder) with spherical and cubical outer bodies using all fluids.
2. $Nu_B = 0.248\ Ra_B^{*0.248}$	15.80	All fluids and inner bodies using a cubical outer body.
3. $Nu_B = 0.578\ Ra_B^{*0.239}$	14.49	All fluids and outer bodies using a cylindrical inner body.
4. $Nu_L = 0.188\ Ra_L^{*0.282}$	18.67	Same as equation 1.
5. $Nu_L = 0.151\ Ra_L^{*0.295}$	17.74	Same as equation 3.

Results of fit to these equations for current data:

DATA	EQUATION 1		EQUATION 2		EQUATION 3		EQUATION 4		EQUATION 5	
	Avg % Dev.	Max % Dev.	Avg % Dev.	Max % Dev.	Avg % Dev.	Max % Dev.	Avg % Dev.	Max % Dev.	Avg % Dev.	Max % Dev.
ALL FLUIDS HORIZONTAL	11.77	24.17	7.966	22.06	7.760	20.82	17.11	34.94	16.78	36.77
ALL FLUIDS VERTICAL	28.91	41.81	22.27	36.04	24.76	38.14	9.785	30.42	9.310	32.81
ALL DATA	20.34	41.81	15.12	36.04	16.26	38.14	13.45	34.94	13.04	36.77

CHAPTER V.

CONCLUSIONS AND RECOMMENDATIONS

This study was initiated primarily to extend the data available for heat transfer in enclosures to more complex inner body geometries. Previous investigations by Bishop [18], Scanlan [19], Warrington [14], and Weber [17] provide a complete analysis of common single body shapes. This investigation has expanded that area by determining the natural convection heat transfer between a set of four isothermal cylinders and a cubical enclosure. The results have pointed out the importance of the geometric effects for multiple bodies and the accuracy with which heat transfer can be correlated for many inner and outer body geometric combinations using only a few simple equations.

Of the geometries studied there appeared to be no appreciable effect due to rotation of the inner body about its vertical axis. However, a significant difference was noticed between the vertical and horizontal configuration of the set of cylinders. The vertical position showed a decrease in the heat transferred relative to the horizontal position. This was attributed to a complex interaction between the boundary layer length, the flow patterns which resulted from the geometry, and the cross sectional area exposed to the upward flow. These geometric effects were noticed to decrease with increasing Prandtl number. As the Prandtl number increased the average percent error decreased from approximately 16% to 1.8% depending on the equation form used. Data at the lowest Prandtl number (air) responded to correlations

better when the geometric effect was taken into account by using the boundary layer length as a characteristic dimension whereas correlations for glycerin provided best results using the hypothetical gap width for all inner body positions. The midrange Prandtl number fluids (water and silicone) exhibited nearly identical results for all equation forms. Many equations were developed to correlate the heat transfer data. These have been provided in tabular form and in nearly all cases are accurate to within a few percent. Of most importance is the capability to predict the heat transfer over a wide Prandtl number range and for several geometries. The following equation:

$$Nu_B = 0.277\ Ra_B^{0.274}\ Pr^{0.012} \tag{5.1}$$

provides acceptable results when computing the heat transfer for a set of cylinders to an enclosure. Computational effort can be somewhat reduced by using

$$Nu_B = 0.286\ Ra_B^{0.275} \tag{5.2}$$

with only 1.0% reduction in accuracy. Similar results are available for corresponding equations based on the hypothetical gap width (L).

Using previous correlations, the data were correlated and the average deviations compared. Warrington [14] concluded that equations developed in his investigation could be extended to most geometries within certain limits of Rayleigh number and gap width. In all

equations using the gap width, the data here supported this conclusion with average percent deviations well under those indicated in Table 4.7. Correlations using the boundary layer length proved to be somewhat above the average deviation and again point out the geometric problem involved when multiple bodies are used. Evidence, herein, indicates that any appreciable departure from the geometries studied here and previously, will provide the best results when the correlations based on gap width are utilized.

RECOMMENDATIONS

A logical progression beyond this study would include increasing the number of cylinders and varying their spacing, diameter, and length. This extension would move the applicability of the correlations to direct industrial application. For practical use of the data base for heat transfer in enclosures, consideration of other multiple geometric shapes such as plates needs to be investigated.

The heat transfer problem for bodies in enclosures is associated with a fluid flow problem. In many cases the heat transfer problem can be solved experimentally without a complete understanding of the flow problem. However, as the geometries become more complex, a more detailed study of the fluid problem must be considered.

APPENDICES

APPENDIX I

HEAT LOSSES FROM THE INNER BODY SUPPORT SYSTEM

Since the primary purpose of this study was to determine the heat transfer from four isothermal cylinders a solution for the heat losses attributed to the support system was required. Although this system was designed to be as small as possible the amount of desired instrumentation was the dominant criterion in sizing the support system. As pointed out in Chapter II, all materials used in the construction of the support system were chosen to minimize the heat transfer from that system to the test fluid. Convection, conduction, and radiation losses were considered. Since radiation and conduction losses for air were discussed in Chapter III, only the conduction and convection losses for the other fluids are detailed here.

Initially, it was assumed that only a small amount of heat would be convected from the support system, especially from the support sphere. However, experimental investigation indicates that the sphere was being heated by natural convection from the test fluid in the chamber.

A study was conducted by embedding two thermocouples in the support sphere. The first 0.125 cm from the outer surface and a second 1.5 cm into the sphere. A comparison of the two temperatures indicated that the surface of the sphere was an average of 0.8K hotter than the inside and reached a maximum of 1.1K hotter at higher ΔT's, thus providing evidence that the sphere was heated by the fluid rather than by the support system.

Flow visualization studies also indicated that the sphere was being heated. Figures 4.5 and I.1 show the flow patterns around the support system. Figure 4.5 represents the body in the horizontal position. There was no perceptible fluid movement around the main support stem, the bottom of the sphere, or the top of the sphere. The flow around the rods which connected the cylinder and the sphere can be attributed primarily to the higher speed flow from the cylinder. The flow pattern leaving the top of the lower cylinder was observed to bend toward the sphere. However, this phenomenon appears common as it can be seen in reference [3] where the support system did not interfere with the flow patterns. This is probably caused by the cool air being drawn into the convective plume as described by other similar flow visualization studies [10, 11]. The resulting flow patterns around the upper cylinder indicate that the support sphere did not appreciably affect the overall fluid movement.

Figure I.1 represents the flow pattern in the vertical plane centered between two adjacent vertical cylinders. The flow around the sphere was induced by the higher speed flow which resulted from heating by the cylinders. The center sphere appeared to direct the flow whereas a more turbulent eddy would probably exist in its absence. Although this effect is not completely predictable, the majority of heat transfer occurs within the high speed flow region along the wall of the cylinder and the presence of an eddy in the center of the geometry would

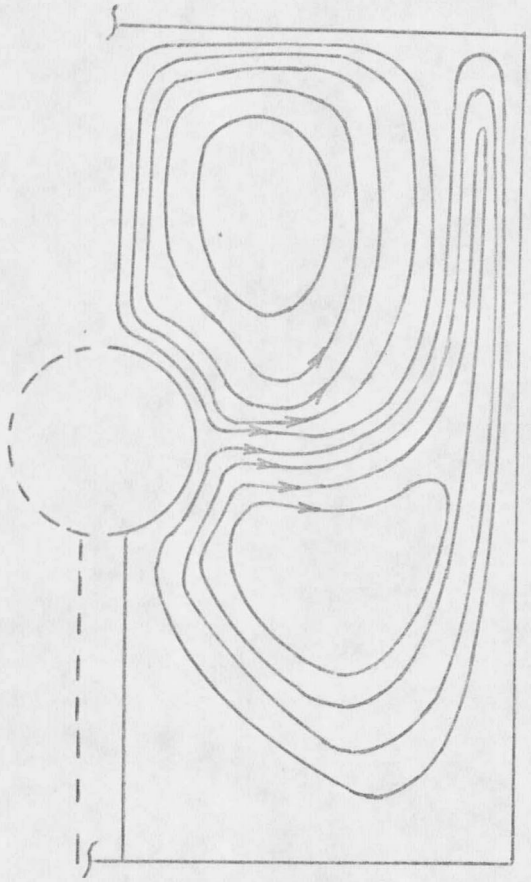


Figure I.1 Flow Pattern Between Cylinders in the Vertical Position.

have little effect on the overall heat transfer as evidenced by previous investigation [14].

These experimental observations and results support the conclusion that the support system is being heated by convection from the cylinders. Therefore, there is little or no heat transfer from the support system to the test fluid. A study of the possible heat loss in the absence of the effects outlined previously presents a major difficulty. However, the following simplified approach indicates that in the absence of heating of the support sphere, less than 0.4% of the total input power would be convected by the sphere. The following assumptions are required in this analysis:

(1) That the sphere is isothermal and its temperature is that measured by the outer surface thermocouple.

(2) That all of the heat leaving the cylinders through the connecting rod is conducted to the sphere.

(3) That the heat leaving the sphere through the main support stem is conducted to the outer body.

From Figure I.2 the resulting heat balance is:

$$Q_{CONV\ OUT} = Q_{COND\ IN} - Q_{COND\ OUT}. \qquad (I.1)$$

The thermal conductivities and areas are known and by using experimental values for the temperatures, $Q_{CONV\ OUT}$ can be calculated. These calculations were carried out and it was determined that

$$\frac{Q_{CONV\ OUT}}{Q_{TOTAL}} \times 100 \leq 0.4\% \quad . \qquad (I.2)$$

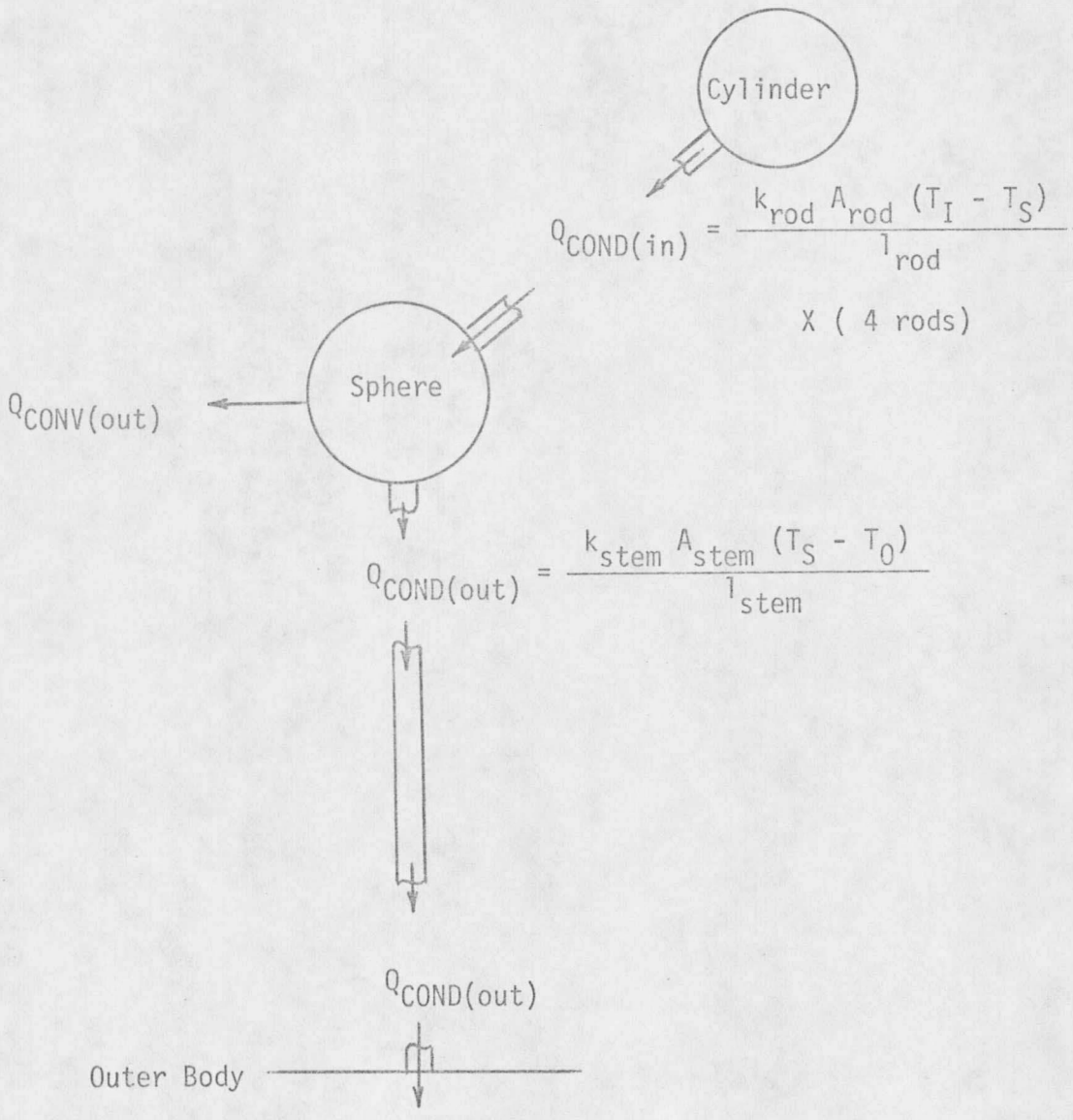


Figure I.2 Steady-State Heat Balance for the Support Sphere.

In the absence of heating of the support sphere the heat transfer from the sphere to the test fluid could be considered negligible.

Conduction heat loss from the test apparatus was calculated using a one-dimensional analysis of the conduction of heat from the support sphere to the outer body through the main support stem and the wiring which it contained. The following equation was used in this calculation:

$$Q_{COND} = \frac{k_s A_s + k_{cc} A_{cc} + k_{htl} A_{htl}}{\Delta l} (T_s - T_o) \qquad (I.3)$$

which was adapted from reference [14]. This correction was not necessary for air since the calibration for radiation losses included the conduction losses through the main support stem.

APPENDIX II

DATA IN THE PARTIALLY REDUCED FORM

The following data were partially reduced using a computer program on the Xerox Sigma VII computer system:

TERMINOLOGY

NGEOM is the body position identifier

NGEOM = 1, Tubes Horizontal and 0^{o} Rotation

NGEOM = 2, Tubes Horizontal and 45^{o} Rotation

NGEOM = 3, Tubes Vertical and 0^{o} Rotation

NGEOM = 4, Tubes Vertical and 45^{o} Rotation

JFI is the fluid identifier

JFI = 1, Air

JFI = 2, 99% Aqueous Glycerin by Weight

JFI = 3, Distilled Water

JFI = 4, Dow Corning Dimethylpolysiloxane (20 centipoise at 25°C)

TAVGI is the average inner body temperature in Kelvin

TAVGO is the average outer body temperature in Kelvin

QCONV is the heat transfer from the tubes by natural convection in Watts

QLOSS is the heat loss due to conduction and radiation in Watts

NGEOM	FJI	TAVGI	TAVGO	QCONV	QLOSS
1	1	300.8911	275.8293	10.8257	4.5495
1	1	320.9531	276.2092	21.8596	8.7719
1	1	320.0317	276.1453	21.2224	8.5714
1	1	335.5232	276.2732	30.6386	12.2767
1	1	369.1121	276.5120	53.6764	21.7092
1	1	291.8083	277.7761	4.8666	2.7856
1	1	351.5647	276.7847	41.0307	16.5462
1	1	312.6440	277.1636	16.3060	6.9135
1	1	326.5227	276.5759	24.8598	10.0692
1	1	360.7214	278.0186	45.6148	19.1301
1	1	341.5488	277.1040	33.8734	13.8197
1	1	294.7517	276.6909	7.0222	3.3645
1	1	306.2866	276.7847	13.0315	5.5967
1	2	303.7593	279.1641	102.0632	1.1178
1	2	290.5134	278.4729	34.4389	.5644
1	2	297.3137	279.4055	64.2133	.8142
1	2	308.8235	281.3201	132.0711	1.2931
1	2	312.6350	280.7588	162.8939	1.4852
1	2	324.9409	284.0703	263.7048	1.9065
1	2	330.9578	286.3162	317.5320	2.0786
1	2	335.0024	288.2358	347.6680	2.1959
1	2	356.3562	294.6887	611.4028	2.8630
1	2	374.7368	299.3350	900.5037	3.4736
1	2	339.8726	289.5476	402.3882	2.3336
1	2	368.4402	298.5015	789.8862	3.2268
1	2	359.7625	291.3179	684.5491	3.1033
1	2	317.3740	281.0544	205.7657	1.6954
1	3	287.1511	279.7654	145.2637	.3934
1	3	295.6953	283.1172	327.2454	.6403
1	3	305.7207	288.7095	569.7917	.8966
1	3	312.4058	292.6829	721.3015	1.0205
1	3	319.2529	296.2654	910.4226	1.1814
1	3	301.8118	286.7583	429.7764	.7678
1	3	291.4773	281.4172	227.9674	.5143
1	4	308.0322	280.0361	201.9373	1.4762
1	4	317.9199	280.7419	301.9424	1.9580
1	4	340.5874	283.6633	531.7197	3.0245
1	4	370.5811	292.4072	829.9453	4.0854
1	4	365.8000	293.6790	743.3945	3.7669
1	4	360.1775	292.6709	679.6592	3.5273
1	4	354.6006	292.4978	610.5542	3.2534
1	4	302.5850	279.6553	160.1241	1.2175
1	4	312.1499	281.0840	239.4488	1.6637

NGEOM	JFI	TAVGI	TAVGO	QCONV	QLOSS
1	4	324.6235	283.6130	343.4346	2.1734
1	4	331.2688	285.6982	393.8181	2.4187
1	4	337.7014	287.3083	457.6252	2.6674
1	4	288.1125	279.8755	43.8588	.4388
1	4	291.7405	280.1040	65.3452	.6070
1	4	296.0330	279.2913	108.3142	.8841
2	1	319.6648	279.9177	23.0483	8.3035
2	1	299.8113	281.1008	8.4386	4.1319
2	1	347.5947	279.5200	44.8582	15.2181
2	1	331.0989	278.0269	33.2602	11.0470
2	1	289.1899	277.6572	4.8014	2.3144
2	1	310.0530	280.1799	15.7129	6.1914
2	1	314.6541	278.4941	20.5415	7.2411
2	1	303.2754	279.5029	11.9163	4.8593
2	1	292.8750	278.9268	6.1841	2.9309
2	2	323.4746	284.1331	244.6227	1.8399
2	2	337.5393	285.8862	389.9072	2.3603
2	2	296.5020	281.8723	52.8402	.6937
2	2	309.4761	280.6448	139.7749	1.3565
2	2	318.1292	284.1836	193.7490	1.6995
2	2	330.6033	286.7375	302.4075	2.0301
2	2	305.2446	283.5879	97.6798	1.0373
2	2	352.3059	289.9326	560.0740	2.8257
2	2	362.9478	293.3992	704.1001	3.1441
2	3	290.4514	282.2388	182.8057	.4304
2	3	293.8064	281.1768	309.6936	.6448
2	3	299.4487	282.3479	494.4407	.8925
2	3	305.3650	285.7651	634.1375	1.0346
2	3	310.4653	287.8286	797.5591	1.1863
2	3	292.9460	281.9902	268.0454	.5735
2	3	296.7964	283.1807	372.1580	.7224
2	3	304.3848	286.7625	558.9868	.9285
2	4	287.3447	279.0793	43.3143	.4401
2	4	296.0232	280.5225	96.5606	.8321
2	4	320.8269	284.5857	293.9106	1.9365
2	4	310.7966	283.4495	200.8837	1.4569
2	4	344.0618	287.3291	527.4548	3.0162
2	4	328.7891	282.3818	396.6091	2.4628
2	4	353.7625	285.9780	664.4192	3.5772
2	4	371.6707	293.5759	829.9480	4.1015
3	1	318.6970	280.2349	13.8114	19.4012
3	1	335.6062	279.9475	22.0749	29.9733
3	1	350.1421	281.0332	28.6585	39.9838

NGEOM	JFI	TAVGI	TAVGO	QCONV	QLOSS
3	1	363.3445	281.2991	35.8345	49.8613
3	1	315.4006	281.1428	11.6626	17.4667
3	1	287.1294	280.8137	1.2154	2.9484
3	1	289.2085	278.7485	3.2904	3.9473
3	1	296.5571	281.3118	3.8881	7.3987
3	1	301.8481	280.5520	6.3676	10.0791
3	1	308.2061	280.0532	9.3484	13.4702
3	1	313.9126	280.3787	11.5619	16.6358
3	1	332.2793	280.3577	20.1363	27.7850
4	1	331.4878	279.3420	20.2283	27.3581
4	1	338.9121	279.5369	23.7913	32.2577
4	1	287.8286	278.6807	2.6401	3.3185
4	1	293.1897	278.8081	4.4281	5.8361
4	1	299.5920	279.2488	6.5169	8.9935
4	1	306.3049	279.6130	8.7636	12.4840
4	1	347.8640	280.2561	28.0481	38.4469
4	1	312.6084	278.7358	12.2537	15.9819
4	1	321.4600	279.9939	15.0014	21.1026
4	1	357.3816	279.9431	33.6312	45.4242
3	2	299.0647	282.6301	67.2570	.8444
3	2	306.3892	282.5583	106.6698	1.2141
3	2	322.6948	285.6233	216.6268	1.8451
3	2	329.7690	287.3833	277.1313	2.0588
3	2	351.9438	292.1392	520.0908	2.8736
3	2	317.5190	286.1411	170.2231	1.5451
3	2	356.3040	289.7793	603.5659	3.1702
3	2	344.4456	290.4128	429.5911	2.6027
3	2	337.0203	290.1853	340.4197	2.2685
3	2	310.7161	282.9326	132.7079	1.3648
4	2	310.4563	282.9746	131.9876	1.3619
4	2	295.6399	277.3340	62.6259	.9001
4	2	303.0332	276.8955	107.7386	1.2999
4	2	339.6428	279.8203	433.8677	2.8463
4	2	349.2419	285.3135	525.2690	3.0003
4	2	314.2004	280.1716	172.4135	1.6599
4	2	320.7068	281.2695	223.6218	1.9189
4	2	327.3267	282.8066	279.1997	2.1456
4	2	333.6094	283.4744	341.1960	2.3929
4	2	355.2383	286.5537	605.6628	3.2239
3	3	301.4688	285.9573	420.6980	.8378
3	3	305.0125	287.5078	506.5647	.9388
3	3	288.7729	281.1851	146.9450	.4298
3	3	291.0964	281.6025	201.1991	.5327

NGEOM	JFI	TAVGI	TAVGO	QCONV	QLOSS
3	3	294.2039	282.6887	265.4355	.6297
3	3	311.0024	288.7380	718.7839	1.1941
3	3	309.2036	289.9534	604.7532	1.0303
3	3	299.4063	286.3120	332.0325	.7019
4	3	312.3911	290.6938	713.4114	1.1699
4	3	310.2861	291.0413	607.6108	1.0336
4	3	307.4050	290.4543	509.3381	.9107
4	3	295.2683	284.1206	263.8301	.5994
4	3	290.4421	283.2729	146.0833	.3999
4	3	292.7297	283.6550	200.8616	.5089
4	3	297.6902	284.4138	335.0520	.7292
4	3	301.1409	285.5645	420.7029	.8429
3	4	290.6375	280.1335	56.1322	.5922
3	4	299.7778	281.5396	108.5977	1.0027
3	4	309.3889	282.6677	179.8355	1.4919
3	4	294.4717	280.1040	80.1735	.7982
3	4	320.0229	283.5542	270.4939	2.0173
3	4	332.3250	285.4182	376.2566	2.5769
3	4	338.8718	286.5081	435.1294	2.8676
3	4	345.7432	287.8032	500.9907	3.1737
3	4	303.4990	281.0417	143.5284	1.2508
3	4	313.9126	282.1628	225.7859	1.7662
3	4	324.8999	283.2393	320.7139	2.2886
3	4	350.8672	287.0830	568.2803	3.5009
3	4	359.8857	290.4001	643.3804	3.8056
3	4	313.6216	281.5437	224.4350	1.7595
4	4	360.7100	290.8716	643.2002	3.8168
4	4	291.4341	280.6196	56.0972	.5953
4	4	299.1226	281.0671	106.4021	1.0082
4	4	308.4937	281.4678	179.8742	1.4766
4	4	319.4910	282.9075	268.9871	2.0068
4	4	331.6375	284.5940	376.3459	2.5782
4	4	312.8015	280.6997	224.6364	1.7675
4	4	296.3948	281.9187	81.3393	.7880
4	4	325.3047	283.4368	321.3735	2.2981
4	4	305.3259	282.8655	144.4204	1.2498
4	4	344.9695	287.2000	499.1257	3.1745

BIBLIOGRAPHY

1. McAdams, W.H., Heat Transmission, Third Ed., McGraw-Hill, New York, 1954, Chapter 7.

2. Gebhart, B., Heat Transfer, Second Ed., McGraw-Hill, New York, 1971, Chapter 8.

3. Holman, J.P., Heat Transfer, Third Ed., McGraw-Hill, New York, 1972, Chapter 7.

4. Fujii, T. and Fujii, M., The Dependence of Local Nusselt Number on Prandtl Number in the Case of Free Convection Along a Vertical Surface with Uniform Heat Flux, International Journal of Heat and Mass Transfer, Vol. 19, pp. 121-122, 1976.

5. Roy, S., High-Prandtl-Number Free Convection for Uniform Surface Heat Flux, Journal of Heat Transfer, Vol. 95, pp. 124-126, 1973.

6. Churchill, S.W. and Ozoe, H., A Correlation for Laminar Free Convection from a Vertical Plate, Transactions of the American Society of Mechanical Engineers, Vol. 95, pp. 540-541, 1973.

7. Leinhard, J.H., On the Commonality of Equations for Natural Convection from Immersed Bodies, International Journal of Heat and Mass Transfer, Vol. 16, pp. 2121-2123, 1973.

8. Eckert, E.R.G. and Soehngen, E., Studies on Heat Transfer in Laminar Free Convection with the Zehnder-Mach Interferometer, Technical Report No. 5747, U.S.A.F. Air Material Command, Dayton, Ohio, 1948.

9. Lieberman, J. and Gebhart, B., Interactions in Natural Convection from an Array of Heated Elements, Experimental, International Journal of Heat and Mass Transfer, Vol. 12, pp. 1385-1396, 1969.

10. Brodowicz, K. and Kierkus, W.T., Experimental Investigation of Laminar Free Convection Flow in Air Above Horizontal Wire with Constant Flux, International Journal of Heat and Mass Transfer, Vol. 9, pp. 81-94, 1966.

11. Forstrom, R.J. and Sparrow, E.M., Experiments on the Buoyant Plume Above a Heated Horizontal Wire, International Journal of Heat and Mass Transfer, Vol. 10, pp. 321-330, 1967.

12. Tillman, E.S., Natural Convection Heat Transfer from Horizontal Tube Bundles, ASME Heat Transfer Conference, August 1976, paper 76-HT-35.

13. Davis, L.P. and Perona, J.J., Development of Free Convection Axial Flow Through a Tube Bundle, International Journal of Heat and Mass Transfer, Vol. 16, pp. 1425-1438, 1973.

14. Warrington, R.O., Natural Convection Heat Transfer Between Bodies and Their Enclosures, Ph.D. Dissertation, Montana State University, 1975.

15. Kuehn, T.H. and Goldstein, R.J., Correlating Equations for Natural Convection Heat Transfer Between Horizontal Circular Cylinders, International Journal of Heat and Mass Transfer, Vol. 19, pp. 1127-1134, 1976.

16. Dutton, J.C. and Welty, J.R., An Experimental Study of Low Prandtl Number Natural Convection in an Array of Uniformly Heated Vertical Cylinders, ASME Heat Transfer Division, February 1975, paper 75-HT-AAA.

17. Weber, N., Natural Convection Heat Transfer Between a Body and its Spherical Enclosure, Ph.D. Dissertation, Montana State University, 1971.

18. Bishop, E.H., Heat Transfer by Natural Convection Between Isothermal Concentric Spheres, Ph.D. Dissertation, University of Texas, Austin, 1964.

19. Scanlan, J.A., Bishop, E.H., and Powe, R.E., Natural Convection Between Concentric Spheres, International Journal of Heat and Mass Transfer, Vol. 13, pp. 1857-1872, 1970.

MONTANA STATE UNIVERSITY LIBRARIES
3 1762 10013383 2

[redacted]

N378
C888
cop.2

Crupper, Gordon
Natural convection heat transfer between a fixed array of cylinders and its cubical enclosure

DATE	ISSUED TO
	Dale Wallace 6/75 [illegible]
	[illegible]
2 WEEKS USE	INTERLIBRARY LOAN
	7-31-85
R	9-2-85

[redacted]

N378
C888
Cop 2